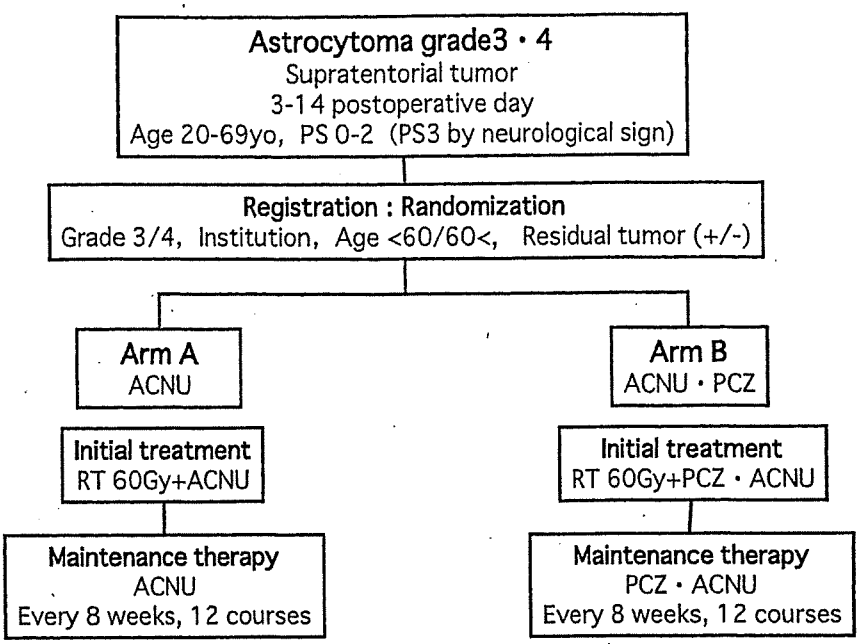

Fig. 3 Scheme of the JCOG 0305 protocol entitled "A randomized phase II / III study of ACNU versus procarbazine plus ACNU as a postoperative chemoradiotherapy for astrocytoma grade 3 and 4." The purpose of this study is to establish a standard therapy for malignant gliomas in Japan.

response 11例（19.0%）という治療効果を得ている．

平成14年度厚生労働科学研究費の助成を受け，「悪性脳腫瘍の標準的治療法の確立に関する研究」班が結成され，JCOG脳腫瘍研究グループとして多施設共同試験を開始するにあたり，悪性グリオーマの標準治療としてはACNUを併用した放射線治療とし，これと比較する新治療としてprocarbazineを先行投与したACNU静注および局所放射線照射として第II/III相試験を計画した（Fig. 3）．対象は20～69歳までのテント上星細胞腫grade 3および4（退形成性星細胞腫および膠芽腫）で，手術により組織診断が確定されたECOG performance status（PS）0，1，2，および腫瘍による神経症状に起因するPS 3症例で，術後14日以内に登録し，ランダム化する．A群としては，放射線照射第1日目および36日目にACNU 80 mg/m^{2}を静脈内投与し，さらに8週ごとに同様の化学療法を12コース行う．B群では，放射線照射第1日目および第36日目より10日間procarbazine 80 mg/m^{2}を経口投与し，服用8日目にACNU 80 mg/m^{2}を静脈内投与する．これもその後8週ごとに12コース繰り返す．放射線治療はCTによる3次元治療計画に基づいて行い，摘出腔および残存腫瘍に2 cmのマージンをつけた領域に60 Gy，MRIのT2強調画像＋2 cmの領域に50 Gyの照射を行う．本臨床試験は，B群の安全性有効性が確立していないため，第II/III相試験として計画されている．すなわち，ランダム化して試験を開始するが，B群症例が56例集積した段階で，安全性有効性を評価し，従来の他の報告に比べ著しく劣っていなければ，そのまま第III相試験に移行し，5年間で310例の症例を集積し，2年間の経過観察期間を設けた後，primary endpointを生存期間，secondary endpointを無増悪生存期間，奏効割合，有害事象として評価される．

従来国内で行われていた多施設共同試験では，エビデンスとなりうるデータを獲得するための条件が揃っているとはいえなかった．エビデンスレベルの高い臨床試験を行うためには，①治療計画コンセプトが科学的な根拠に基づくものであり，②そのコンセプトに基づいたプロトコールを作成し，③施設内の治験審査委員会（institutional review board；IRB）の承認を取得する．さらに，④患者本人に病状，治療法，効果などについて十分な説明を行ったうえでの同意（IC）を得て，⑤プロトコールに沿った治療を実施する．⑥集められたデータについては，その信頼性を確認するための監査機関を設け，⑦結果に対して何ら先入観を持たない第三者による統計解析を行い，⑧その結果を学会誌等に発表するというプロセスが必要である．

Table 3 Taylor-made chemotherapy for malignant gliomas

1. Selection of drugs unrelated to chemoresistant genes	
Gene	Related drugs
MDR-1	adriamycin, vincristine, cyclophosphamide, methotrexate
MRP-1	adriamycin, etoposide
MRP-2	etoposide, cisplatin
TOPO II α	etoposide, adriamycin
MGMT	nitrosourea
GST-π	cisplatin
2. Pretreatment with drugs with anti-chemoresitance	
O^6-benzylguanine or procarbazine against MGMT	
3. Selection of drugs with high sensitivity	
PCV (PAV) therapy for anaplastic oligodendroglioma with 1p/19q loss	

テーラーメイド治療

大規模臨床試験が，多くの症例に同一の治療をして，より有効な治療法を探索していこうという方法をとっているのに対し，テーラーメイド治療とは，個々の腫瘍に対して，薬剤感受性・耐性に関連する情報に基づいた薬剤を選択し，至適な治療を行っていくものであり，相反する治療法といえる．現時点では，ある形質を持つ腫瘍に対して，この治療法を選択すれば治癒できるというものがないため，厳密な意味でのテーラーメイド治療は存在しない．しかしながら，わずかでも有効な治療法を選択して治療効果を高めようという努力がなされている．その方法としてはまず，耐性のない薬剤の選択ということで，いわば消極的なテーラーメイド治療である．これは，薬剤耐性の遺伝子や酵素の有無を各腫瘍について調べ，例えば，多剤耐性遺伝子 multidrug resistance (MDR)-1 が発現していれば，adriamycin, vincristine, cyclophosphamide, methotrexate などを選択しない，MGMT が高値の場合は ACNU 等の nitrosourea 系薬剤を用いないという方法である[6)7)12)16)] (Table 3)．この場合，それ以外の薬剤が感受性を示すという保証はないばかりでなく，国内で使用できる薬剤の制約により，臨床応用が困難であるという問題がある．次に，MGMT を消費し枯渇させて nitrosourea 系薬剤の感受性を高める方法で，O^6-benzylguanine や procarbazine などを nitrosourea に先立って投与する方法であるが，これについてはまだ十分なエビデンスはなく，前述した procarbazine＋ACNU による臨床試験の結果が俟たれる．悪性脳腫瘍に対して，比較的実用化の進んでいるテーラーメイド治療は，退形成性乏突起膠腫に対する procarbazine＋CCNU＋vincrsitine (PCV) 療法（国内では CCNU の代わりに ACNU が用いられるため PAV 療法と呼ばれることが多い）である．これは多くの退形成性乏突起膠腫に染色体 1p および 19q の欠失があり，その大半が PCV 療法に反応するという報告に基づくものである．遺伝子異常と治療法が密接に結びついた貴重な報告であり，今後このような発見が多く出てくることが期待される[3)10)]．しかしながら，この治療法自体は臨床研究としては前期第 II 相レベルであり，これによって退形成性乏突起膠腫の治療法が決定した訳ではなく，特に国内で行われている PAV 療法は PCV 療法と同様な効果が得られるという保証はない．臨床的には広く実施され，多くの有効例があるとされているが，本来は第III相試験まで行い，その有効性を確認することが望ましい．

おわりに
—臨床試験とテーラーメイド療法の接点—

ある一定の形質を持った腫瘍に対し，特定の治療法がきわめて有効な場合，テーラーメイド治療は必須なものである．しかしながら，現時点では標的とされている形質が存在し，その形質に対する特定の治療を行っても，いかなる種類の悪性グリオーマも治癒は困難である．治療成績を改善するためには，一つひとつ有効と思われる治療法の効果を検証していく必要があり，その判断材料が臨床試験ということになろう．そのような検証の中から，単に「MGMT 陽性」とか「1p 欠失」とか狭い範囲の形質に対して有効な治療というものではなく，「膠芽腫」あるいは「悪性グリオーマ」という形質に対して有効な治療法が確立されていくことが望まれる．

文　献

1) Anderson AP: Postoperative irradiation of glioblastomas. *Acta Radiol Oncol Radiat Phys Biol* 17: 475-484, 1978.
2) Brandes AA, Turazzi S, Basso U, Pasetto LM, Guglielmi B, Volpin L, Iuzzolino P, Amista P, Pinna G, Scienza R, Ermani M: A multidrug combination designed for reversing resistance to BCNU in glioblastoma multiform. *Neurology* 58: 1759-1764, 2002.
3) Cairncross JG, Ueki K, Zlatescu MC, Lisle DK, Finkslestein DM, Hammond RR, Silver JS, Stark PC, Macdnald DR, Ino Y, Ramsay DA, Louis DN: Specific genetic predictors of chemotherapeutic response and survival in patients with anaplastic oligodendrogliomas. *J Natl Cancer Inst* 90: 1473-1479, 1998.
4) Chang CH, Horton J, Schoenfeld D, Salezer O, Perez-Tamayo R, Kramer S, Weinstein A, Nelson JS, Tukada Y: Comparison of postoperative radiotherapy and combined

postoperative radiotherapy and chemotherapy in the multidisciplinary management of malignant gliomas. *Cancer* 52：997-1007, 1983.
5) Committee of Brain Tumor Registry of Japan：Report of Brain Tumor Registry of Japan (1969-1996). *Neurol Med chir* 43：1-111, 2003.
6) Fojo AT, Ueda K, Slamon DJ, Poplack DG, Gottesman MM, Pastan I：Expression of a multidrug resistance gene in human tumors and tissues. *Proc Natl Acad Sci* 84：265-269, 1987.
7) Grant CE, Valdimarsson G, Hipfner DR, Almquist KC, Cole SP, Deeley RG：Overexpression of multidrug resistance-associated protein (MRP) increases resistance to natural product drug. *Cancer Res* 54：357-361, 1994.
8) Green SB, Byar DP, Walker MD, Pistenmaa DA, Alexander E Jr, Batzdorf U, Brooks WH, Hunt WE, Maeley J Jr, Odom GL, Paoletti P, Ransohoff J 2nd, Robertson JT, Selker RG, Shapiro WR, Smith KR Jr, Wilson CB, Strike TA：Comparisons of carmustine, procarbazine and high-dose methylprednisolone as additions surgery and radiotherapy for the treatment of malignant gliomas. *Cancer Treat Rep* 67：121-132, 1983.
9) Hensley ML, Schuchter LM, Lindley C, Meropol NJ, Cohen GI, Broder G, Gradishar WJ, Green DM, Langdon RJ Jr, Mitchell RB, Negrin R, Szatrowski TP, Thigpen JT, Von Hoff D, Wasserman TH, Winer EP, Pfister DG：American Society of Clinical Oncology clinical practice guidelines for the use of chemotherapy and radiotherapy protectants. *J Clin Oncol* 17：3333-3355, 1999.
10) Ino Y, Betensky RB, Zlatescu MC, Sasaki H, Macdonald DR, Stemmer-Rachamimov AO, Ramsay DA, Cairncross JG, Louis DN：Molecular subtypes of anaplastic oligodendroglioma：Implications for patient managament at diagnosis. *Clin Cancer Res* 7：839-845, 2001.
11) 嘉山孝正：転移性脳腫瘍に対する標準的治療法確立に関する研究. 平成16年度厚生労働科学研究　がん臨床研究成果発表会抄録集. 長寿科学振興財団, 2005, pp.42-45.
12) Pegg AE：Mammalian O^6-alkylguanine-DNA alkyltransferase：Regulation and importance in response to alkylating carcinogenic and therpeutic agents. *Cancer Res* 50：6119-6129, 1990.
13) Shibui S：A randomized controlled trial on malignant brain tumors. The activities of Japan Clinical Oncology Group (JCOG) -Brain Tumor Study Group (BTSG). *Neurol med chir* 44：220-221, 2004.
14) 渋井壮一郎：悪性脳腫瘍の標準的治療法の確立に関する研究. 平成16年度厚生労働科学研究　がん臨床研究成果発表会抄録集. 長寿科学振興財団, 2005, pp.34-36.
15) 篠田　淳, 矢野大仁, 坂井　昇：悪性グリオーマの治療成績：これまでのエビデンス. 脳外誌 13：3-19, 2004.
16) Silber JR, Bobola MS, Ghatan S, Blank A, Kolstoe DD, Berger MS：O^6-methylguanine-DNA methyltransferase activity in adult gliomas：Relation to patient and tumor characteristics. *Cancer Res* 58：1068-1073, 1998.
17) Takakura K, Abe H, Tanaka R, et al：Effects of ACNU and radiotherapy on malignant glioma. *J Neurosurg* 64：53-57, 1986.
18) Valavanis C, Souliotis VL, Kyrtopoulos SA：Differential effects of procarbazine and methylnitrosourea on the accumulation of O^6-methylguanine and the depletion and recovery of O^6-alkylguanine-DNA alkyltransferase in rat tissues. *Carcinogenesis* 15：1681-1688, 1994.
19) Walker MD, Strike TA, Sheline GE：An analysis of dose-effect relationship in the radiotherapy of malignant gliomas. *Int J Radiat Oncol Biol Phys* 5：1725-1731, 1979.
20) Walker MD, Green SB, Byar DP, Alexander E Jr, Batzdorf U, Brooks WH, Hunt WE, MacCarty CS, Mahaley MS Jr, Mealey J Jr, Owens G, Ransohoff J 2nd, Robertson JT, Shapiro WR, Smith KR Jr, Wilson CB, Strike TA：Randomized comparisons of radiotherapy and nitrosoureas for the treatment of malignant glioma after surgery. *N Engl J Med* 303：1323-1329, 1980.
21) Winger MJ, Macdonald DR, Cairncross JG：Supratentorial anaplastic gliomas in adults. The prognostic importance of extent of resection and prior low-grade glioma. *J Neurosurg* 71：487-493, 1989.

要　旨

悪性グリオーマに対する化学療法
—大規模臨床試験とテーラーメイド治療—

渋井壮一郎

国内における悪性グリオーマの標準治療を確立する目的で，厚生労働科学研究費の助成を受けて，2002年にJCOG脳腫瘍研究グループが設立され，国内で一般的に行われているACNU+放射線治療に対し，procarbazine+ACNU+放射線照射の治療効果を検証する第Ⅱ/Ⅲ相試験が開始された．エビデンスとなりうる臨床試験を実施するためには，信頼できるデータ管理機構を持つ多施設共同試験が必須である．薬剤耐性や感受性など，個々の腫瘍の持つ形質を考慮したテーラーメイド治療も各種試みられているが，それらがエビデンスレベルの高い治療法として確立されるためには，臨床試験の積み重ねが必要となる．

脳外誌　15：3-9，2006

Acta Neuropathol (2006) 111: 483–488
DOI 10.1007/s00401-006-0063-y

ORIGINAL PAPER

Kazuhiko Mishima · Yukinari Kato · Mika Kato Kaneko
Ryo Nishikawa · Takanori Hirose · Masao Matsutani

Increased expression of podoplanin in malignant astrocytic tumors as a novel molecular marker of malignant progression

Received: 30 January 2006 / Revised: 22 February 2006 / Accepted: 6 March 2006 / Published online: 5 April 2006

Abstract Podoplanin (aggrus) is a mucin-like transmembrane sialoglycoprotein that is expressed on lymphatic endothelial cells. Podoplanin is putatively involved in cancer cell migration, invasion, metastasis, and malignant progression and may be involved in platelet aggregation. Previously, we showed upregulated expression of podoplanin in central nervous system (CNS) germinomas, but not in non-germinomatous germ cell tumors, except for parts of immature teratomas in limited numbers. However, little information exists about its role in CNS astrocytic tumors. In this study, 188 astrocytic tumors (30 diffuse astrocytomas, 43 anaplastic astrocytomas, and 115 glioblastomas) were investigated using immunohistochemistry with an anti-podoplanin antibody, YM-1. In 11 of 43 anaplastic astrocytomas (25.6%) and in 54 of 115 glioblastomas (47.0%), podoplanin was expressed on the surface of anaplastic astrocytoma cells and glioblastoma cells, especially around necrotic areas and proliferating endothelial cells. However, the surrounding brain parenchyma was not stained by YM-1. On the other hand, podoplanin expression was not observed in diffuse astrocytoma (0/30: 0%). Furthermore, we investigated the expression of podoplanin using quantitative real-time PCR and Western blot analysis in 54 frozen astrocytic tumors (6 diffuse astrocytomas, 14 anaplastic astrocytomas, and 34 glioblastomas). Podoplanin mRNA and protein expression were markedly higher in glioblastomas than in anaplastic astrocytomas. These data suggest that podoplanin expression might be associated with malignancy of astrocytic tumors.

Keywords Podoplanin · Astrocytoma · Glioblastoma · YM-1

K. Mishima · R. Nishikawa · M. Matsutani
Department of Neurosurgery, Saitama Medical School,
38 Morohongo Moroyama-machi Iruma-gun,
Saitama 350-0495, Japan

Y. Kato (✉) · M. K. Kaneko
Research Center for Glycoscience,
National Institute of Advanced Industrial Science and
Technology (AIST), Open Space Laboratory C-2,
1-1-1 Umezono, Tsukuba, Ibaraki 305-8568, Japan
E-mail: yukinari-k@bea.hi-ho.ne.jp
Tel.: +81-29-8613197
Fax: +81-29-8613191

T. Hirose
Department of Pathology, Saitama Medical School,
38 Morohongo Moroyama-machi Iruma-gun,
Saitama 350-0495, Japan

Introduction

Astrocytic tumors are the most common tumors of the central nervous system (CNS) and are categorized into diffuse astrocytomas (World Health Organization (WHO) Grade II), anaplastic astrocytomas (AA; WHO Grade III) and glioblastomas (GBM; WHO Grade IV) [11]. Among them, GBMs are the most frequent and most malignant type of astrocytic tumor. Despite advances in surgical techniques, radiation therapy, and adjuvant chemotherapy, their prognosis remains poor: the median survival time for patients with GBMs is only 1 year [2]. Glioblastoma may occur de novo or may result from progression of low-grade astrocytomas [4]. Molecular mechanisms of tumorigenesis and malignant progression are associated with the inactivation of tumor suppressor genes such as p53-Rb pathway or the overexpression of oncogenes such as epidermal growth factor receptor [10]. However, the mechanisms of tumorigenesis and progression of astrocytic tumors have not been resolved. Identification of genes that are expressed differentially in high-grade astrocytomas, low-grade tumors, or normal brain tissues is important to elucidate the molecular mechanisms of tumorigenesis and to develop novel therapeutic strategies.

Podoplanin was reported to be expressed in lymphatic endothelium and in tumor-associated lymphangiogenesis; also, podoplanin deficiency resulted in congenital lymphedema and impaired lymphatic vascular patterning [16]. Furthermore, expression of podoplanin has been

shown to be upregulated in skin squamous cell carcinoma [12], lung squamous cell carcinoma [9], malignant mesothelioma [14], Kaposi's sarcoma, angiosarcoma [1], hemangioblastoma [15], testicular seminoma [7, 8], and dysgerminoma [17].

We have recently shown that podoplanin is overexpressed in CNS germinomas, but not in non-germinomatous germ cell tumors, except in a limited number of immature teratomas with partial positive reactivity [13]. In adult non-neoplastic CNS, podoplanin was evident in the subependymal areas, the leptomeninges, choroid plexus, ependyma, and Purkinje cells [15, 17]. However, podoplanin expression in CNS astrocytic tumors has not been studied intensively. In this study, we investigated podoplanin expression in 188 astrocytic tumors.

Materials and methods

Tissue samples

Tumor specimens were obtained during surgery from eight patients with diffuse astrocytomas, 14 patients with anaplastic astrocytomas, and 34 patients with glioblastomas. Informed consent had been obtained previously from patients or their guardians. The tumor specimens were routinely fixed in 10% buffered formalin for 18–20 h at room temperature and processed to paraffin. Sections (5 μm thick) were cut and attached to poly-L-lysine-coated glass slides. Hematoxylin-eosin was used for routine staining. Tissue microarrays of 132 astrocytic tumors (22 diffuse astrocytomas, 29 anaplastic astrocytomas, and 81 glioblastomas) were purchased from Cybrdi, Inc. (Frederick, MD). The histology of these tissue samples was confirmed by experienced neuropathologists.

Immunohistochemical analysis

Specimens were deparaffinized, rehydrated, and incubated first with YM-1 (1/100 diluted; Medical Biological Laboratories Co., Ltd, Nagoya, Japan) at room temperature for 1 h, then with biotin-conjugated secondary anti-rat IgG antibody (DakoCytomation, Glostrup, Denmark) for 1 h, and finally with peroxidase-conjugated biotin–streptavidin complex (Vectastain ABC Kit; Vector Laboratories, Inc., Burlingame, CA) for 1 h. Color was developed using 3,3-diaminobenzidine tetrahydrochloride tablet sets (DakoCytomation) for 3 min. Podoplanin expression was assessed semi-quantitatively from the percentage of tumor cells with cytoplasmic/membrane staining: 0, no staining; +, <10%; ++, 10–50%; and +++, >50%.

Western blot analysis

Tissues were solubilized with lysis buffer (25 mM Tris (pH 7.4), 50 mM NaCl, 0.5% Na deoxycholate, 2% nonidet P-40, 0.2% SDS, 1 mM phenylmethylsulfonyl fluoride, and 50 mg/ml aprotinin). They were then electrophoresed under reducing conditions on 10–20% polyacrylamide gels (Daiichi Pure Chemicals Co., Ltd, Tokyo, Japan). The separated proteins were transferred to a nitrocellulose membrane. After blocking with 4% skim milk in PBS, the membrane was incubated with YM-1 (1/500 diluted) or anti-β-actin antibody (1 μg/ml; Sigma Chemical Co., St. Louis, MO), and then with peroxidase-conjugated secondary antibodies (1/1,000 diluted; Amersham Pharmacia Biotech UK Ltd, Buckinghamshire, UK). The proteins were subsequently developed for 3 min using ECL reagents (Amersham Pharmacia Biotech) using X-Omat AR film (Eastman Kodak Co.).

Quantitative real-time PCR

Total RNAs were prepared from frozen sections that have been obtained from astrocytic tumor patients, employing an RNeasy mini prep kit (Qiagen, Inc., Hilden, Germany). The initial cDNA strand was synthesized using SuperScript III transcriptase (Invitrogen Co., Carlsbad, CA) by priming nine random oligomers and an oligo-dT primer according to the manufacturer's instructions. We performed PCR using oligonucleotides: human podoplanin sense (5′-GGAAGGTGTCAGCT CTGCTC-3′) and human podoplanin antisense (5′-CG CCTTCCAAACCTGTAGTC-3′). Real-time PCR was carried out using the QuantiTect SYBR Green PCR (Qiagen, Inc.). The PCR conditions were 95°C for 15 min (1 cycle), followed by 40 cycles of 94°C for 15 s, 53°C for 20 s, 72°C for 10 s. Subsequently, a melting curve program was applied with continuous fluorescence measurement. A standard curve for podoplanin templates was generated through serial dilution of PCR products (1×10^8–1×10^2 copies/μl). The expression level of podoplanin was normalized by total RNA weights. The statistical signifi cance of podoplanin mRNA expression in astrocytic tumor tissues was determined using paired *t* tests.

Results

Immunohistochemical staining for podoplanin in malignant astrocytic tumors

The cellular distribution of podoplanin in astrocytic tumors was examined immunohistochemically using anti-podoplanin antibody, YM-1, which can strongly recognize podoplanin [6, 13]. In this study, we used 56 surgical tissues (8 diffuse astrocytomas, 14 anaplastic astrocytomas, and 34 glioblastomas). Podoplanin immunoreactivity was detected in 5 of 14 (35.7%) anaplastic astrocytomas and in 18 of 34 (52.9%) glioblastomas; staining was graded as +++ in 16 glioblastomas and as ++ in two glioblastoma cases. We also stained other astrocytic tumors of tissue microarrays. Podoplanin was detected in 6 of 29 (21%) anaplastic astrocytomas and in 36 of 81 (44%) glioblastomas. In all, 11 of 43 anaplastic

astrocytomas (25.6%) and 54 of 115 (47.0%) glioblastomas were stained using YM-1 (χ^2, $P<0.05$; Table 1). Representative staining for podoplanin in glioblastoma samples is shown in Fig. 1. Immunostaining for podoplanin demonstrated predominantly cell surface patterns in glioblastoma cells (Fig. 1). In anaplastic astrocytoma, the tumor cell surface was stained using YM-1 (Fig. 1c, d). In glioblastomas, podoplanin-positive tumor cells were prominent around microvascular proliferations (Fig. 1e, f) and necrotic tissues (Fig. 1g). Proliferating endothelial cells were negative for podoplanin (Fig. 1e, f). Podoplanin was detected strongly in the plasma membrane of highly anaplastic multinucleated giant cells (Fig. 1h). In non-neoplastic areas of the brain (Fig. 1a) and in diffuse astrocytoma (Fig. 1b), podoplanin immunostaining was absent.

Podoplanin expression in malignant astrocytic tumors using Western blot analysis

To confirm immunohistochemical findings from astrocytic tumors, lysates of frozen tumor specimens from 54 patients (6 diffuse astrocytomas, 14 anaplastic astrocytomas, and 34 glioblastomas) were analyzed using Western blotting. As shown in Fig. 2, an antibody to podoplanin, YM-1, detected about 36-kDa proteins in extracts of malignant astrocytomas. Using YM-1, 6 of 14 anaplastic astrocytomas (42.8%) and 22 of 34 glioblastomas (64.7%) showed strong labeling (χ^2, $P<0.05$), while all diffuse astrocytomas were negative. Podoplanin expression detected by Western blot analysis was closely correlated with the results of immunohistochemistry.

Differential expression of podoplanin mRNA in astrocytic tumors

To quantify the expression of podoplanin mRNA in human astrocytic tumors of different grades, we performed quantitative real-time PCR analyses of astrocytic tumors from 54 patients (6 diffuse astrocytomas, 14 anaplastic astrocytomas, and 34 glioblastomas). The relative podoplanin mRNA expression levels of each tumor grade are shown in Fig. 3. Average copies of podoplanin mRNA/μg total RNA in diffuse astrocytomas (Grade II), anaplastic astrocytomas (Grade III), and glioblastomas (Grade IV) were 21.7±30.6, 16.1±35.4, and 411.2±511.7, respectively. Podoplanin transcript levels were significantly higher in glioblastomas than those in diffuse astrocytomas, anaplastic astrocytomas, or non-neoplastic human brain tissues ($P<0.01$).

Discussion

Immunohistochemical, Western blot, and real-time PCR analyses demonstrate that the expressions of podoplanin mRNA and protein are correlated with the malignant progression from anaplastic astrocytoma (Grade III) to glioblastomas (Grade IV). Of particular interest, 47.0% of highly invasive glioblastomas express podoplanin, whereas 25.6% of anaplastic astrocytomas and 0% of the less invasive diffuse astrocytomas (Grade II) express podoplanin by immunohistochemical staining on surgically resected and microarray tissues (Table 1). On the other hand, 6 of 14 anaplastic astrocytomas (42.8%) and 22 of 34 glioblastomas (64.7%) were strongly labeled by Western blot analyses using YM-1 (Fig. 2). Of all 188 astrocytic tumors analyzed immunohistochemically, 132 cases were derived from tissue microarrays whose tissue spots are small and, therefore, the percentage of podoplanin-positive tumors might have been underestimated. Furthermore, YM-1 detected podoplanin strongly by Western blot analysis, as described previously [6]. For these reasons, podoplanin-positive ratios in immunohistochemical analysis are inferred to be smaller than those of Western blot analysis, although the expression of podoplanin detected by immunohistochemistry was closely correlated with that by Western blot or real-time PCR analyses. The distribution of podoplanin-positive tumor cells was prominent around necrotic tissue and proliferating endothelial cells in glioblastomas (Fig. 1). Normal brain tissue surrounding the tumor bed was negative for podoplanin. Therefore, podoplanin expression was correlated with high tumor grades and aggressive histological behavior.

The biological functions of podoplanin remain largely unknown. In vascular endothelial cells, overexpression of T1α/podoplanin induces elongated cell extensions and considerably increases cell adhesion, migration, and tube

Table 1 Results of podoplanin immunostaining in 188 patients with astrocytic tumors

Tumor type	No. of cases	Podoplanin immunostaining				Positive rate (%)
		+++	++	+	–	
Diffuse astrocytoma	30	0	0	0	30	0
Surgical resection samples	8	0	0	0	8	0
Tissue microarray	22	0	0	0	22	0
Anaplastic astrocytoma	43	6	3	2	32	25.6
Surgical resection samples	14	3	1	1	9	35.7
Tissue microarray	29	3	2	1	23	20.7
Glioblastoma	115	39	10	5	61	47
Surgical resection samples	34	16	2	0	16	52.9
Tissue microarray	81	23	8	5	45	44

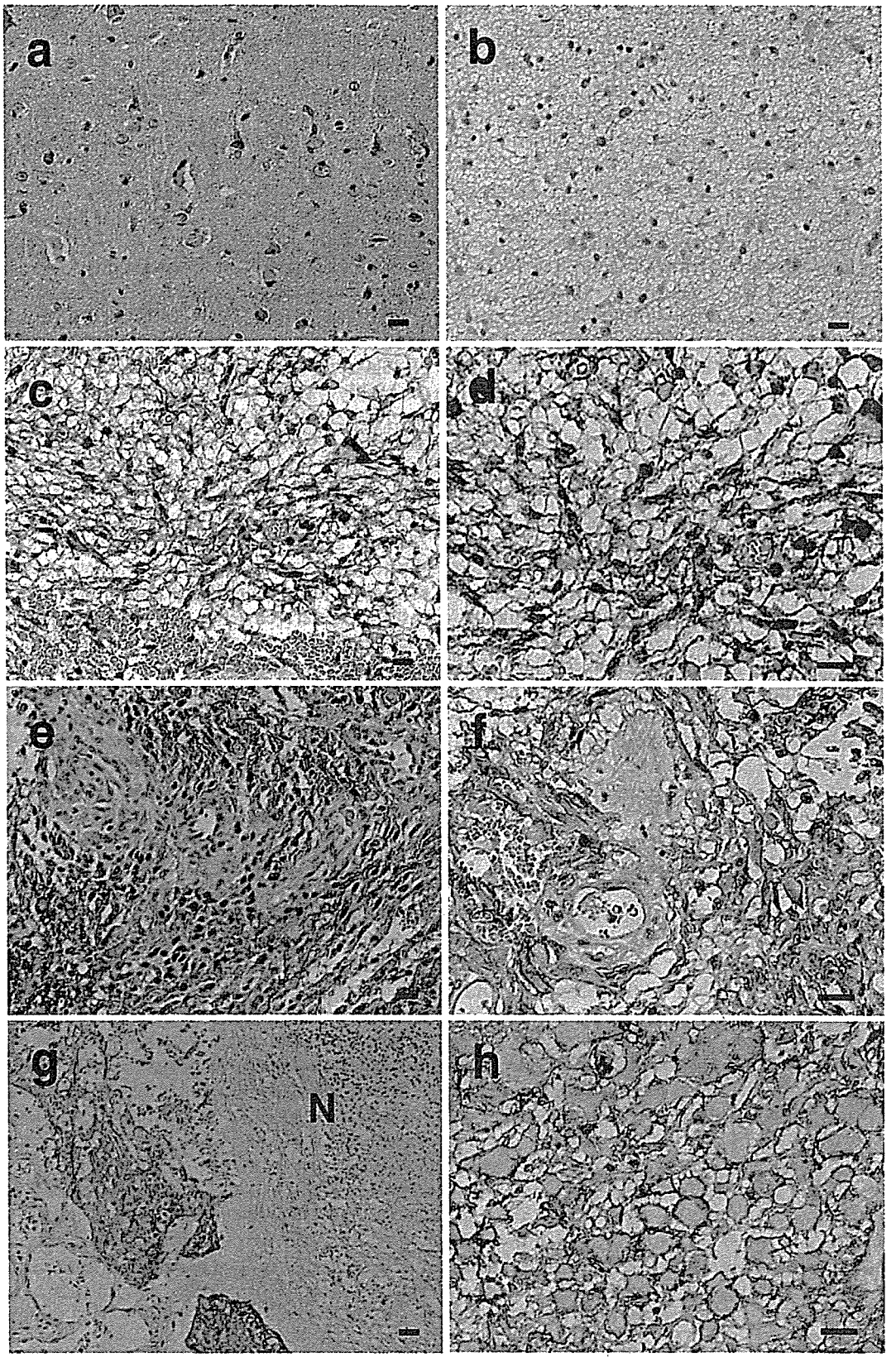

Fig. 1 Immunohistochemical detection of podoplanin in astrocytic tumors. No staining is apparent in a normal brain (**a**, ×200) and in diffuse astrocytoma (**b**, ×200). In anaplastic astrocytoma, the tumor cell surface was stained positively (**c**, ×200; **d**, ×400). Accentuated staining is visible around an area of microvascular proliferation in glioblastoma (**e**, ×200; **f**, ×400). Podoplanin immunostaining of glioblastoma cells at the necrotic area (*N*) (**g**, ×200) and in the plasma membrane of highly anaplastic multinucleated giant cells (**h**, ×400). *Bar*=10 μm

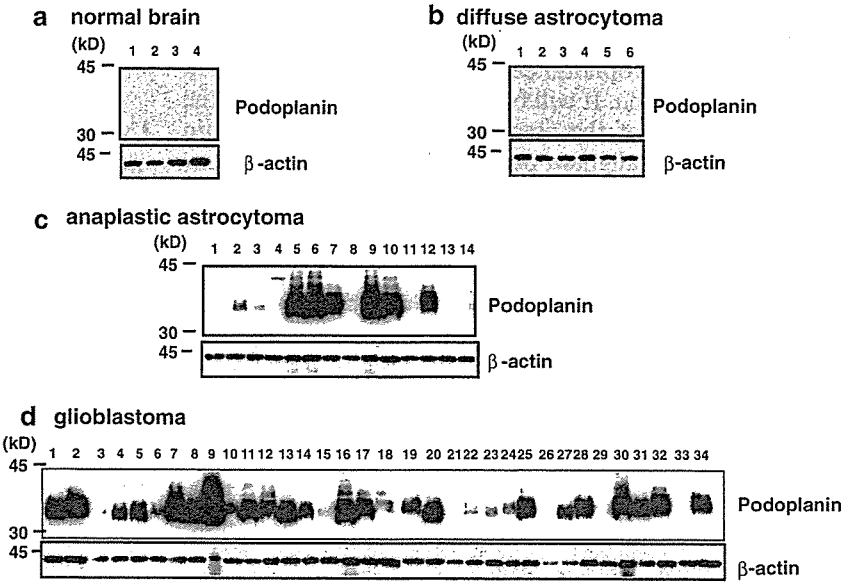

Fig. 2 Western blot analyses of podoplanin expression in astrocytic tumors. Tissues from normal brain (**a**), diffuse astrocytomas (**b**), anaplastic astrocytomas (**c**), and glioblastomas (**d**) were solubilized and immunoblotted using anti-human podoplanin monoclonal antibody YM-1 (*upper panel*) or anti-β-actin antibody (*lower panel*)

formation by promoting the rearrangement of the actin cytoskeleton [16]. PA2.26/podoplanin was identified as a cell surface protein induced in epidermal carcinogenesis and skin remodeling [18, 19]. Expression of PA2.26/podoplanin in pre-malignant keratinocytes induces a fully transformed and metastatic phenotype. Furthermore, human PA2.26/podoplanin has been found in the invasive front of oral squamous cell carcinomas, consistent with a role in tumor cell migration and invasion [12]. Moreover, a monoclonal antibody against gp44/aggrus/podoplanin inhibits pulmonary metastasis of a highly metastatic clone of mouse colon adenocarcinoma in vivo [21, 22]. In this study, we showed upregulated expression of podoplanin in CNS malignant astrocytic tumors. Recently, Shibahara et al. [20] also reported podoplanin expression in subsets of CNS tumors. However, the results obtained so far showed only associations between podoplanin expression and malignancy of astrocytic tumors, while its direct biological function in malignant astrocytomas remains to be established.

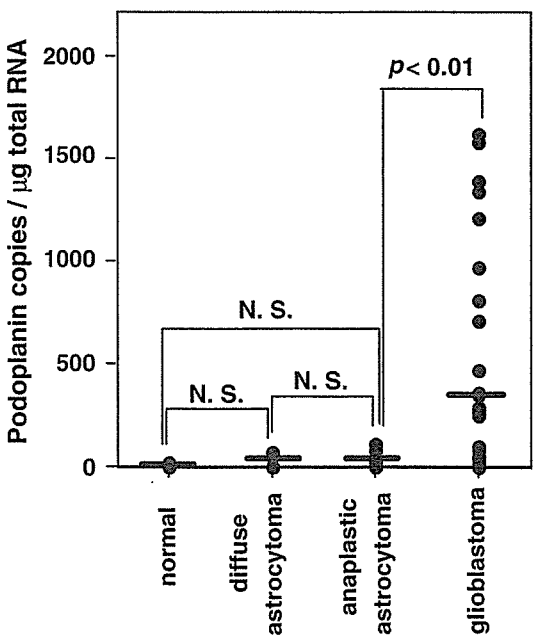

Fig. 3 Quantitative real-time PCR analysis of podoplanin transcripts in astrocytic tumors. First-strand cDNA samples derived from astrocytic tumor tissues of 54 patients (6 diffuse astrocytomas, 14 anaplastic astrocytomas, and 34 glioblastomas) and four normal brain tissues were used as real-time PCR templates. The respective expression levels of podoplanin were normalized to μg or total RNA, as described in Materials and methods

PA2.26/podoplanin was co-localized with ezrin, radixin, moesin family proteins, which are concentrated in cell surface projections, where they link the actin cytoskeleton to plasma membrane proteins [18]. Consistent with the association of podoplanin with ezrin, the latter's immunoreactivity is also associated with increasing malignancy of astrocytic tumors [3, 23]. The combination of podoplanin and ezrin might thus represent a possible tool for grading of astrocytic tumors.

Platelets play an important role in hemostasis and thrombosis and are also involved in tissue repair and tumor metastasis [5]. Glioblastoma is differentiated from low-grade astrocytomas based on the histological presence of tumor necrosis and associated microvascular proliferation [11]. Large necroses are attributable to insufficient blood supply and thrombosed tumor vessels are often observed. We speculate that the local platelet aggregation and thrombus formation might be increased by podoplanin-expressing malignant astrocytic tumor cells, resulting in tumor vessel obstruction and subsequent necrosis. Indeed, our unpublished results suggest that podoplanin expressed by glioblastoma cells induces platelet aggregation in vitro (data not shown).

In conclusion, podoplanin expression was markedly higher in glioblastomas than in anaplastic astrocytomas. Furthermore, podoplanin expression was not observed in diffuse astrocytoma. It will be intriguing to investigate the functional basis of the association between podoplanin expression and malignant progression of astrocytomas.

Acknowledgments This study was supported in part by Kanae Foundation for Life and Socio-medical Science (to Y.K.) and by Osaka Cancer Research Foundation (to Y.K.). We thank Drs Fujita and Tsuruo (University of Tokyo) for their great help, and Ms Kunita, Mr Nakazawa (University of Tokyo), Ms Totake, and Ms Kobo (Saitama Medical School) for their kind assistance. We thank Dr Sugiyama (Hiroshima University) for providing us clinical samples.

References

1. Breiteneder-Geleff S, Soleiman A, Kowalski H, Horvat R, Amann G, Kriehuber E, Diem K, Weninger W, Tschachler E, Alitalo K, Kerjaschki D (1999) Angiosarcomas express mixed endothelial phenotypes of blood and lymphatic capillaries: podoplanin as a specific marker for lymphatic endothelium. Am J Pathol 154:385–394
2. DeAngelis LM (2001) Brain tumors. N Engl J Med 344:114–123
3. Geiger KD, Stoldt P, Schlote W, Derouiche A (2000) Ezrin immunoreactivity is associated with increasing malignancy of astrocytic tumors but is absent in oligodendrogliomas. Am J Pathol 157:1785–1793
4. Giese A, Bjerkvig R, Berens ME, Westphal M (2003) Cost of migration: invasion of malignant gliomas and implications for treatment. J Clin Oncol 21:1624–1636
5. Honn KV, Tang DG, Crissman JD (1992) Platelets and cancer metastasis: a causal relationship? Cancer Metastasis Rev 11:325–351
6. Kaneko M, Kato Y, Kunita A, Fujita N, Tsuruo T, Osawa M (2004) Functional sialylated O-glycan to platelet aggregation on Aggrus (T1alpha/podoplanin) molecules expressed in Chinese Hamster Ovary cells. J Biol Chem 279:38838–38843
7. Kato Y, Fujita N, Kunita A, Sato S, Kaneko M, Osawa M, Tsuruo T (2003) Molecular identification of Aggrus/T1alpha as a platelet aggregation-inducing factor expressed in colorectal tumors. J Biol Chem 278:51599–51605
8. Kato Y, Sasagawa I, Kaneko M, Osawa M, Fujita N, Tsuruo T (2004) Aggrus: a diagnostic marker that distinguishes seminoma from embryonal carcinoma in testicular germ cell tumors. Oncogene 23:8552–8556
9. Kato Y, Kaneko M, Sata M, Fujita N, Tsuruo T, Osawa M (2005) Enhanced expression of Aggrus (T1alpha/podoplanin), a platelet-aggregation-inducing factor in lung squamous cell carcinoma. Tumor Biol 26:195–200
10. Kleihues P, Ohgaki H (1999) Primary and secondary glioblastomas: from concept to clinical diagnosis. Neuro-oncology 1:44–51
11. Kleihues P, Burger PC, Collins VP, Newcomb EW, Ohgaki H, Cavenee WK (2000) Astrocytic tumors. Glioblastoma. In: Kleihues P, Cavenee WK (eds) Pathology and genetics of tumours of the nervous system. International Agency for Research on Cancer Press, Lyons, France, pp 29–39
12. Martin-Villar E, Scholl FG, Gamallo C, Yurrita MM, Munoz-Guerra M, Cruces J, Quintanilla M (2005) Characterization of human PA2.26 antigen (T1alpha-2, podoplanin), a small membrane mucin induced in oral squamous cell carcinomas. Int J Cancer 113:899–910
13. Mishima K, Kato Y, Kaneko KM, Nakazawa Y, Kunita A, Fujita N, Tsuruo T, Nishikawa R, Hirose T, Matsutani M (2006) Podoplanin expression in primary central nervous system germ cell tumors: a useful histological marker for the diagnosis of germinoma. Acta Neuropathol (Berl) (in press)
14. Ordonez NG (2005) D2-40 and podoplanin are highly specific and sensitive immunohistochemical markers of epithelioid malignant mesothelioma. Hum Pathol 36:372–380
15. Roy S, Chu A, Trojanowski JQ, Zhang PJ (2005) D2-40, a novel monoclonal antibody against the M2A antigen as a marker to distinguish hemangioblastomas from renal cell carcinomas. Acta Neuropathol (Berl) 109:497–502
16. Schacht V, Ramirez MI, Hong YK, Hirakawa S, Feng D, Harvey N, Williams M, Dvorak AM, Dvorak HF, Oliver G, Detmar M (2003) T1alpha/podoplanin deficiency disrupts normal lymphatic vasculature formation and causes lymphedema. EMBO J 22:3546–3556
17. Schacht V, Dadras SS, Johnson LA, Jackson DG, Hong YK, Detmar M (2005) Up-regulation of the lymphatic marker podoplanin, a mucin-type transmembrane glycoprotein, in human squamous cell carcinomas and germ cell tumors. Am J Pathol 166:913–921
18. Scholl FG, Gamallo C, Vilaro S, Quintanilla M (1999) Identification of PA2.26 antigen as a novel cell-surface mucin-type glycoprotein that induces plasma membrane extensions and increased motility in keratinocytes. J Cell Sci 112:4601–4613
19. Scholl FG, Gamallo C, Quintanilla M (2000) Ectopic expression of PA2.26 antigen in epidermal keratinocytes leads to destabilization of adherens junctions and malignant progression. Lab Invest 80:1749–1759
20. Shibahara J, Kashima T, Kikuchi Y, Kunita A, Fukayama M (2006) Podoplanin is expressed in subsets of tumors of the central nervous system. Virchows Arch (in press)
21. Sugimoto Y, Watanabe M, Oh-hara T, Sato S, Isoe T, Tsuruo T (1991) Suppression of experimental lung colonization of a metastatic variant of murine colon adenocarcinoma 26 by a monoclonal antibody 8F11 inhibiting tumor cell-induced platelet aggregation. Cancer Res 51:921–925
22. Tsuruo T, Yamori T, Naganuma K, Tsukagoshi S, Sakurai Y (1983) Characterization of metastatic clones derived from a metastatic variant of mouse colon adenocarcinoma 26. Cancer Res 43:5437–5442
23. Tynninen O, Carpen O, Jaaskelainen J, Paavonen T, Paetau A (2004) Ezrin expression in tissue microarray of primary and recurrent gliomas. Neuropathol Appl Neurobiol 30:472–477

Human Pathology (2006) 37, 627–630

ELSEVIER

Human PATHOLOGY

www.elsevier.com/locate/humpath

Papillary glioneuronal tumor with minigemistocytic components and increased proliferative activity

Takashi Ishizawa MD[a,*], Takashi Komori MD[b], Junji Shibahara MD[d], Keisuke Ishizawa MD[a], Jun-ichi Adachi MD[c], Ryo Nishikawa MD[c], Masao Matsutani MD[c], Takanori Hirose MD[a]

[a]*Department of Pathology, Saitama Medical School, Moroyama, Iruma-gun, Saitama 350-0495, Japan*
[b]*Department of Clinical Neuropathology, Tokyo Metropolitan Institute for Neuroscience, Tokyo 183-8526, Japan*
[c]*Department of Neurosurgery, Saitama Medical School, Moroyama, Iruma-gun, Saitama 350-0495, Japan*
[d]*Department of Human Pathology, University of Tokyo Graduate School of Medicine, Tokyo 113-0033, Japan*

Received 6 September 2005; accepted 20 December 2005

Keywords:
Papillary glioneuronal tumor;
Minigemistocyte;
Immunohistochemistry;
Ultrastructure

Summary Papillary glioneuronal tumor (PGNT) is a rare and new type of glioneuronal neoplasm of the central nervous system. It is characterized by pseudopapillary structures composed of hyalinized vessels rimmed by cuboidal glial cells and the proliferation of neuronal cells. We report a peculiar PGNT arising in the parietal lobe of a 67-year-old man, which was characterized by proliferation of minigemistocytic cells as well as typical components. The minigemistocytic cells had eccentric nuclei and plump eosinophilic cytoplasm that was filled with glial filaments. The Ki-67 labeling index was as high as 10% in the minigemistocytic areas. Recently, the presence of oligodendroglial-like component was suggested in PGNT. Considering that oligodendroglioma sometimes accompanies minigemistocytic components, the minigemistocytic cells in PGNT were suggested to be a part of oligodendroglial differentiation. Although PGNT is defined as an indolent glioneuronal tumor, the presence of minigemistocytic components with the high Ki-67 labeling index may indicate more aggressive nature.

1. Introduction

Papillary glioneuronal tumor (PGNT) is a rare brain tumor that shows mixed neuronal and glial differentiation, first reported by Komori et al [1] in 1998. Papillary glioneuronal tumor typically occurs in the periventricular hemispheres of young people [2] and appears to be a variable-sized, contrast-enhancing cystic mass with calcification by radiographic imaging studies [1,3,4]. Histologically, PGNT displays compact pseudopapillae composed of hyalinized vessels covered by glial fibrillary acidic protein (GFAP)–positive astrocytes and variable-sized synaptophysin-positive neuronal cells, including neurocytes, ganglioid cells, and ganglion cells with neuropils [1]. Ki-67 labeling index has been reported to be low, indicating that the tumor has a low proliferative activity. Recently, we experienced an extraordinary PGNT characterized by a proliferation of

* Corresponding author. Saitama Medical School, Morohonngou 38, Moroyama, Iruma-gun, Saitama, Japan.
E-mail address: tishi@saitama-med.ac.jp (T. Ishizawa).

0046-8177/$ – see front matter © 2006 Elsevier Inc. All rights reserved.
doi:10.1016/j.humpath.2005.12.014

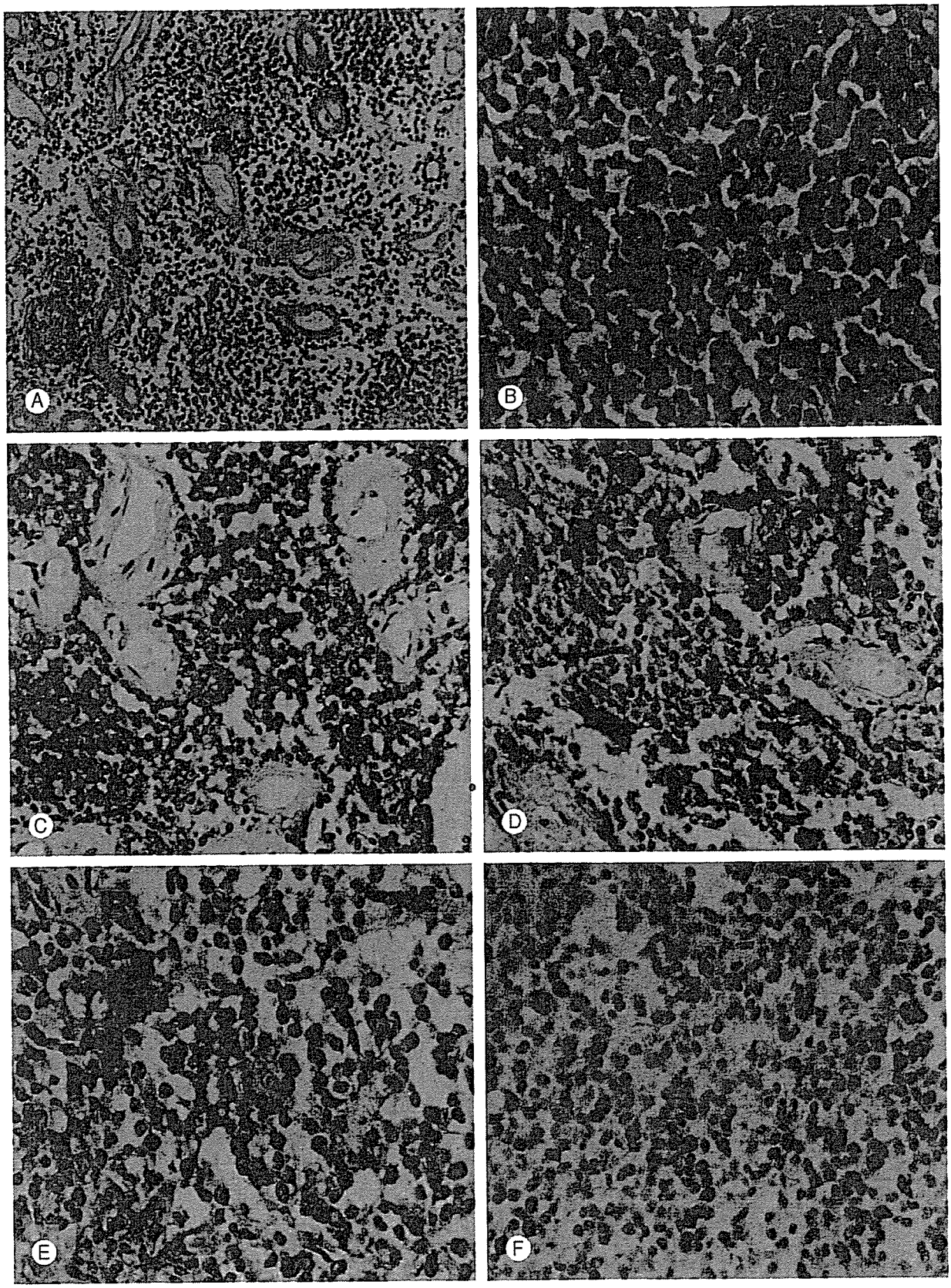

Fig. 1 Light microscopic features of PGNT. (A) Pseudopapillary structures composed of small hyalinized blood vessels. Small neuronal cells are present between papillae. (B) Minigemistocytic cells with brightly eosinophilic cytoplasm and eccentrically located nuclei. (C) Neurocytic cells exhibiting synaptophysin immunoreactivity. (D) GFAP-positive cells surrounding hyalinized vessels. (E) Minigemistocytic cells with immunoreactivity for GFAP. (F) Ki-67 immunoreactivity in minigemistocytic areas.

round-shaped cells, morphologically consistent with minigemistocytic cells. The aim of this article is to study the minigemistocytic component of this PGNT with immunohistochemical and ultrastructural methods.

2. Case report

A 67-year-old man was admitted in our hospital because of a recurrent brain tumor. Eleven years ago, he presented with left hemiparesis and was diagnosed as having "angioma" in the right parietal region by an magnetic resonance imaging examination and brain biopsy. He was followed up without medical intervention for about 10 years after the first diagnosis. As his hemiparesis began to deteriorate recently and his brain tumor grew larger, he was referred to our hospital. On magnetic resonance imaging examination, the tumor was 2.5 cm in diameter and showed cystic areas with gadolinium enhancement. Partial resection of the tumor was undertaken, and postoperative radiochemotherapy was carried out to residual tumor; however, he showed clinical signs of regrowth 6 months after the surgery.

3. Pathological findings

The original biopsy specimens, reviewed by one of us (J.S.), showed small amount of pseudopapillary structures in addition to many hyalinized blood vessels with hemosiderin deposition. Unfortunately, pseudopapillary areas were lost in the newly prepared sections for the present study.

The tumor obtained at partial resection was uniquely characterized by a pseudopapillary pattern (Fig. 1A). The pseudopapillary structures were composed of hyalinized blood vessels and were lined, predominantly, by a single layer of ovoid to cuboidal cells, which had small pyknotic nuclei. In the intervening regions between the pseudopapillae, small round cells with a high nuclear cytoplasm ratio proliferated diffusely. These round cells were relatively uniform in appearance and possessed round nuclei with a prominent nucleolus and fine granular cytoplasm, mimicking neurocytes. In addition to these histologic features, there were some areas showing diffuse proliferation of ovoid cells, which lacked cell processes (Fig. 1B). They were characterized by brightly eosinophilic cytoplasm and eccentrically located nuclei. In the cytoplasm, small filamentous inclusion-like bodies were often noted, which displaced or indented the nuclei. These features indicated the similarities between these cells and minigemistocytes or "mini-" rhabdoid cells. Variable amount of minigemistocyte-like cells were also seen between neurocytic cells. In spite of high cellularity of minigemistocytic cells, neither necrosis nor endothelial proliferation was noted in the specimens, and mitoses were difficult to demonstrate. At the periphery of the lesions, there were gliotic areas with hemosiderin deposition and clusters of collapsed vessels with calcification.

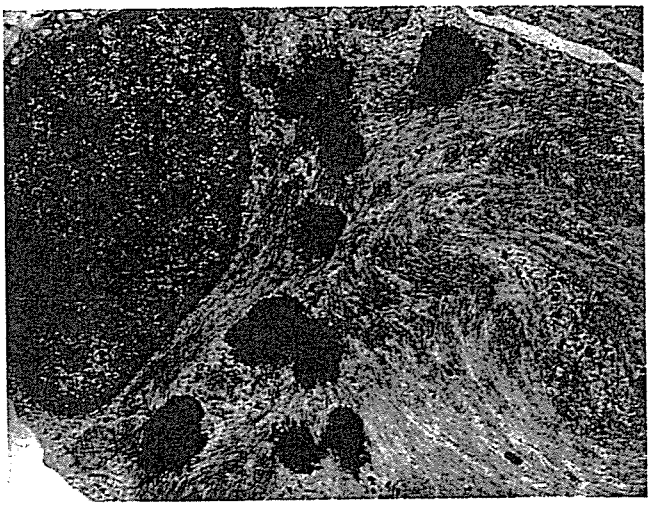

Fig. 2 Ultrastructural features of minigemistocytic cells. The cytoplasm is filled with abundant bundles of intermediate filaments, which are associated with amorphous, Rosenthal fiber-like electron-dense materials.

Immunohistochemically, small neurocytic cells scattered in interpseudopapillary areas were positive for synaptophysin (Fig. 1C), neurofilament, neuron-specific enolase, neuronal class III β-tubulin, chromogranin A, NeuN, and S-100 protein but negative for cytokeratin, epithelial membrane antigen, and p53 protein. The cuboidal cells around the vascular cores were GFAP- (Fig. 1D) and S-100 protein–positive and negative for neuronal markers, revealing that these cuboidal cells show astrocytic differentiation. The minigemistocyte-like cells were also GFAP- and S-100 protein–positive (Fig. 1E) and negative for neuronal markers. The Ki-67 labeling index was low in the pseudopapillary area; however, in areas composed of diffuse proliferation of minigemistocytic cells, the index was as high as 5% to 10%, suggesting that the minigemistocytic cells had a high proliferative activity (Fig. 1F).

Only the minigemistocytic components were included in the materials for ultrastructural study. Minigemistocyte-like cells had ovoid or indented nuclei and wide cytoplasm. The latter was often filled with abundant bundles of intermediate filaments, which displaced the nuclei to the periphery of cytoplasm (Fig. 2). Occasionally, small amorphous, electron-dense materials were included within the filaments. As the dense materials were closely associated with intermediate filaments, they seemed to correspond to Rosenthal fibers (Fig. 2). Cell processes were poorly developed.

4. Discussion

Nine cases of PGNT have been reported in the original paper and 13 cases have been subsequently reported to our knowledge [2,5-11]. Histologically, the tumor consists of 2 characteristic components: pseudopapillary component

composed of cuboidal cells covering hyalinized vessels and diffuse proliferation of small to middle-sized round cells in a sheet-like fashion [1]. The perivascular cuboidal cells are GFAP-positive, suggesting astrocytic differentiation. The small to middle-sized round cells are synaptophysin- and neurofilament-positive [1], implying that they show neuronal differentiation. Clinicopathologically, the tumor occurs in relatively younger people [1-3,5,6,8-11]; however, some elderly cases were also reported [7,11]. The cerebral hemisphere is the common location of the tumor where it shows contrast-enhancing variable-sized cystic masses [1,9]. As no recurrence was experienced during the follow-up period in the original paper, PGNT has been recognized as a benign or indolent lesion.

The present tumor fulfilled the pathological criteria of PGNT. Furthermore, our case possessed peculiar cell components, that is, eosinophilic round cells mimicking "mini" rhabdoid cells. Distinctive cellular features such as cell roundness, eosinophilic cytoplasm, eccentric nuclei, GFAP-immunoreactivity, aggregates of intermediate filaments, and intracytoplasmic Rosenthal fibers suggest the similarities between these cells and minigemistocytes, which are often noted in oligodendrogliomas. They proliferated diffusely and intermingled with neurocytic cells in the present case. Although Komori et al ultrastructurally demonstrated "nonspecific" cells, diffuse proliferation of minigemistocytic cells has not been described in their original paper.

Recently, Olig2-positive cellular components have been demonstrated in PGNT. Olig2 is a transcription factor that regulates the development of oligodendrocytes and specifies the cellular phenotype of oligodendrocytes [11]. Tanaka et al [11] studied 6 PGNTs including the present case (their case no. 2) and revealed Olig2 expression in all of them. Based on the results, they speculated the participation of oligodendroglial components in PGNT [11] in addition to neuronal and astrocytic cells. Although Olig2 expression is not always specific to oligodendroglial lineage [12], considering that oligodendrogliomas often accompany minigemistocytes, oligodendroglial components can potentially be a third constitutional element of PGNT. Thus, the present case seems to be an interesting PGNT with prominent minigemistocytic differentiation.

Although PGNT is considered to be an indolent lesion, our case included areas with a high proliferative activity (a high Ki-67 labeling index). The tumor was partially resected and treated by radiochemotherapy; however, after 6 months from the surgery, the tumor showed tendency of regrowth. Initially, the tumor remained stable for almost 10 years only with the biopsy and then started the recognizable growth. Considering the microscopic features and Ki-67 labeling index, the minigemistocytic areas seem to correspond to proliferating elements. The present case may indicate the possibility of transformation of PGNT in a more aggressive phase. Because the number of PGNT cases reported is still small, the biologic behavior and clinical outcome with long follow-up periods are undetermined yet.

In summary, we experienced a PGNT with proliferation of minigemistocytic component, which showed a high proliferative activity, suggesting cellular and biologic diversities of PGNT.

References

[1] Komori T, Scheithauer BW, Anthony DC, et al. Papillary glioneuronal tumor: a new variant of mixed neuronal-glial neoplasm. Am J Surg Pathol 1998;22:1171-83.
[2] Broholm H, Madsen FF, Wagner AA, et al. Papillary glioneuronal tumor a new tumor entity. Clin Neuropathol 2002;21:1-4.
[3] Cenacchi G, Giangaspero F. Emerging tumor entities and variants of CNS neoplasms. J Neuropathol Exp Neurol 2004;63:185-92.
[4] McLendon RE, Provenzale J. Glioneuronal tumors of the central nervous system. Brain Tumor Pathol 2002;19:51-8.
[5] Ebato M, Tsunoda A, Maruki C, et al. Papillary glioneuronal tumor with highly degenerative pseudopapillary structure accompanied by specific abortive glial cells: a case report. No Shinkei Geka 2003;31:1185-90.
[6] Lamszus K, Makrigeorgi-Butera M, Laas R, et al. September 2002: 24-year-old female with a 6-month history of seizures. Brain Pathol 2003;13:115-7.
[7] Tsukayama C, Arakawa Y. A papillary glioneuronal tumor arising in an elderly woman: a case report. Brain Tumor Pathol 2002;19:35-9.
[8] Prayson RA. Papillary glioneuronal tumor. Arch Pathol Lab Med 2000;124:1820-3.
[9] Bouvier-Labit C, Daniel L, Dufour H, et al. Papillary glioneuronal tumour: clinicopathological and biochemical study of one case with 7-year follow up. Acta Neuropathol (Berl) 2000;99:321-6.
[10] Kordek R, Hennig R, Jacobsen E, et al. Papillary glioneuronal tumor a new variant of benign mixed brain neoplasm. Pol J Pathol 2003;54:75-8.
[11] Tanaka Y, Yokoo H, Komori T, et al. A distinct pattern of Olig2-positive cellular distribution in papillary glioneuronal tumors: a manifestation of the oligodendroglial phenotype? Acta Neuropathol 2005;110:39-47.
[12] Yokoo H, Nobusawa S, Takebayashi H, et al. Anti-human Olig2 antibody as a useful immunohistochemical marker of normal oligodendrocytes and gliomas. Am J Pathol 2004;164:1717-25.

Available online at www.sciencedirect.com
ScienceDirect
Biochemical and Biophysical Research Communications 349 (2006) 277–283
BBRC
www.elsevier.com/locate/ybbrc

Brain- and heart-specific *Patched-1* containing exon 12b is a dominant negative isoform and is expressed in medulloblastomas ☆

Hideki Uchikawa [a,b], Masashi Toyoda [a], Kazuaki Nagao [a], Hiroshi Miyauchi [c], Ryo Nishikawa [c], Katsunori Fujii [b], Yoichi Kohno [b], Masao Yamada [a], Toshiyuki Miyashita [a,*]

[a] *Department of Genetics, National Research Institute for Child Health and Development, Tokyo 157-8535, Japan*
[b] *Department of Pediatrics, Graduate School of Medicine, Chiba University, Chiba 260-8670, Japan*
[c] *Department of Neurosurgery, Saitama Medical School, Saitama 350-0495, Japan*

Received 31 July 2006
Available online 17 August 2006

Abstract

Mutations in the human tumor suppressor gene, *Patched-1*, are associated with nevoid basal cell carcinoma syndrome characterized by developmental abnormalities and tumorigenesis, such as basal cell carcinoma and medulloblastoma. During the investigation of complex alternative splicing in *Patched-1*, we identified an alternative exon, exon 12b, located between exon 12 and 13, both in humans and in mice. Since exon 12b has an in-frame stop codon, the mRNA isoform containing this exon (*Patched12b*) encodes a truncated patched-1 protein. RT-PCR and whole mount *in situ* hybridization revealed that mouse exon 12b was expressed in the brain and heart, particularly in the cerebellum, in both adults and embryos. We next performed a functional analysis of *Patched12b* using a GLI-responsive luciferase reporter. Luciferase activity was suppressed when transfected with a plasmid encoding *Patched-1*, but not with a plasmid for *Patched12b*. The suppressive activity of Patched-1 was relieved when cotransfected with a plasmid for *Patched12b*. This implies that the Patched12b protein has a dominant negative effect on Patched-1. Interestingly, *Patched12b* was found to be expressed in some of the medulloblastoma tissues and cell lines, indicating an important role in the pathogenesis of medulloblastoma as well as brain development.

Keywords: Alternative splicing; Medulloblastoma; Nevoid basal cell carcinoma syndrome; Patched-1

The *Patched-1* gene (*Ptc1*) controls cell growth and specification of the developing and postnatal tissues of many animals [1]. The nevoid basal cell carcinoma syndrome (NBCCS), also called Gorlin syndrome, is associated with mutations in a human *Ptc1* homolog, *PTCH* [2,3]. NBCCS is an autosomal dominant neurocutaneous disorder characterized by developmental malformations, such as syndactyly and spina bifida, and an increased incidence of a variety of tumors, including basal cell carcinoma (BCC) and medulloblastoma [4]. Mutations of *PTCH* are also detected in a small fraction of holoprosencephaly characterized by a failure of the complete separation of the forebrain into right and left halves [5]. Heterozygous loss of *PTCH* found in certain sporadic and familial cases of BCC and medulloblastoma indicates that *PTCH* is also a tumor suppressor gene [6–8]. Ptc1, a 12-pass transmembrane protein, is the ligand-binding component of the receptor complex for a secreted protein, Sonic hedgehog (Shh). In the absence of Shh binding, Ptc1 is thought to hold Smoothened (Smo), another component of the Shh receptor, in an inactive state and thus inhibit signaling to

☆ *Abbreviations:* AS, alternative splicing; BCC, basal cell carcinoma; EGFP, enhanced green fluorescent protein; NBCCS, nevoid basal cell carcinoma syndrome; NMD, nonsense-mediated mRNA decay; PTC, premature termination codon; Shh, Sonic hedgehog.

* Corresponding author. Fax: +81 3 5494 7035.
E-mail address: tmiyashita@nch.go.jp (T. Miyashita).

0006-291X/$ - see front matter © 2006 Elsevier Inc. All rights reserved.
doi:10.1016/j.bbrc.2006.08.046

downstream genes. Upon the binding of Shh, the inhibition of Smo is released and signaling is transduced, leading to the activation of target genes by the Gli family of transcription factors [1].

We and others have identified a number of *PTCH* mRNA isoforms generated by alternative splicing (AS) [9–11]. Among these isoforms, the one containing exon 12b conserved in both humans and mice (*PTCH12b* and *Ptcl2b*, respectively) is particularly interesting since it is expressed in a brain- and heart-specific fashion, at least in human tissues [12]. Here, we show that mouse *Ptcl2b* is also preferentially expressed in the brain and in the heart. Since this isoform has an in-frame stop codon, it encodes truncated Ptc1, which does not seem to have any functions. However, the functional analysis of this isoform demonstrated that it functions as a dominant negative isoform against Ptc1. Furthermore, *PTCH12b* was found to be expressed in some of the medulloblastoma tissues and cell lines, indicating an important role in the pathogenesis of medulloblastomas as well as brain development.

Materials and methods

Constructs. The plasmids for myc-PTCH and 8 × GLI-Luc were kindly provided by Dr. J. Ming and Dr. S. Ishii, respectively. Mouse *Ptc1* cDNA sequence, exon 12-12b-13, was amplified by RT-PCR. The primers used for the amplification were 5′-TTCTCCCTCCAGTACTGATG-3′ (exon 12 forward), 5′-CACCACAGCAGCCTTGGGAG-3′ (exon 13 reverse). The PCR product was subcloned into pGEM-T Easy (Promega) and used for *in situ* hybridization. pMyc-PTCH and pMyc-PTCH12b were described previously [12]. To produce pPTCH-EGFP and pPTCH12b-EGFP, *PTCH* sequences for exon 1a-exon23 and exon 1a-exon12b, respectively, were amplified by PCR using pMyc-PTCHM or pMyc-PTCH12b as a template and subcloned into pEGFP-N3 (Clontech). The primers used for the amplification were 5′-GGGGTACCGCTATGGGGAAGGCTA CTGG-3′ (exon 1a-2 forward), 5′-CGGGATCCGTTGGAGCTGCTT CCCCGGG-3′ (exon 23 reverse), and 5′-CGGGATCCCTCCTCG TAAGGAAACCTCATGTA-3′ (exon 12b reverse). Restriction enzyme recognition sequences (underlined) were added to facilitate subcloning.

RT-PCR. Total RNA was extracted using the RNeasy kit from Qiagen according to the manufacturer's recommendations. RT-PCR was performed as previously described using 5 μg of total RNA [11]. Primers used for RT-PCR were 5′-TGGCCCATGCATTCAGTGAAACA-3′ (mouse exon 11 forward), 5′-GAGGGTCATACTCTGTGCGGA-3′ (mouse exon 14 reverse), 5′-GTGTTGGTGTGGATGATGTTT-3′ (human exon 11 forward), and 5′-CGGGATCCTTGTAAAACAGCAGAAAAT-3′ (human exon 13 reverse).

Western blotting. Immunoblot analysis was performed as described previously [13]. In brief, 30 μg of the cell lysate was subjected to SDS–PAGE and transferred onto a nitrocellulose membrane. The membrane was incubated with anti-c-Myc mouse monoclonal antibody (Santa Cruz, 9E10) followed by horseradish peroxidase-conjugated anti-mouse immunoglobulins (DAKO) or with anti-GFP rabbit polyclonal antibody (Medical & Biological Laboratories, Japan) followed by horseradish peroxidase-conjugated anti-rabbit IgG (Santa Cruz).

Luciferase assay. I-23 cells growing on six-well plates were cotransfected using Effectene reagent (Qiagen) with various combinations of plasmids as indicated in Fig. 4. The total amount of transfected DNA was adjusted to 3 μg with an empty plasmid, pcDNA3.0. Twenty-four hours after the transfection, cells were harvested and subjected to the luciferase assay with the reagents and protocols provided by Promega. Firefly luciferase activity was normalized by Renilla luciferase activity from a cotransfected pRL-SV40 (Promega).

In situ hybridization. The plasmids described above were linearized and digoxigenin-labeled cRNA probes were synthesized using T7 or SP6 RNA polymerase. E10.5 embryos on a C57BL/6J background were fixed in 4% paraformaldehyde in PBS, dehydrated in methanol, and stored at −20 °C. For hybridization, embryos were rehydrated in 0.1% Tween 20 in PBS (PBT) and incubated with proteinase K (10 μg/ml in PBT) for 15 min at 37 °C. Digestion was stopped by washing with 2 mg/ml glycine in PBT, and embryos were refixed in 4% paraformaldehyde and 0.25% glutaraldehyde in PBT, washed in PBT, and hybridized overnight at 65 °C with 2 μg/ml of digoxigenin-labeled RNA probes in hybridization solution (50% formamide, 5 × SSC, 2% blocking powder (Roche), 0.1% Tween 20, 0.5% CHAPS, 50 μg/ml yeast RNA, 5 mM EDTA, and 50 μg/ml heparin). Embryos were washed in hybridization solution and in 2 × SSC, 0.1% CHAPS at 65 °C, and incubated for 30 min with 20 μg/ml RNase A in 2 × SSC, 0.1% CHAPS at 37 °C. After washing, embryos were blocked for 3 h in 10% sheep serum, 1% BSA in PBT and incubated overnight at 4 °C with anti-digoxigenin antibody (Roche) (1:2000 diluted in 10% sheep serum, 1% BSA in PBT with 1.5 mg/ml mouse embryo powder). Embryos were washed 5 times in 1% BSA in PBT for 1 h each, 3 times in NTMT (100 mM NaCl, 100 mM Tris–HCl, pH 9.5, 50 mM $MgCl_2$, and 0.1% Tween 20) for 10 min each, and stained with NBT/BCIP stock solution (Roche) (1:50 diluted in NTMT) for about 2 h at room temperature.

Immunostaining and confocal microscopy. Immunostaining was performed essentially as described previously [14]. Briefly, HeLa cells were seeded on chamber slides (Nalge Nunc International) and were transfected with the constructs indicated in the figure legend. After 24 h, the slides were fixed with 4% paraformaldehyde, permeabilized, stained with anti-c-myc antibody (Santa Cruz, 9E10) followed with FITC-labeled anti-mouse immunoglobulins (DAKO), and observed with an Olympus microscope FV300. Nuclear localization was confirmed by Hoechst33342 staining. EGFP fusion proteins were observed as described previously [15].

Results

Tissue-specific regulation of Ptcl2b expression in mice

Previously, we identified a *patched-1* isoform containing a novel exon, exon 12b, between exon 12 and exon 13 both in humans (*PTCH12b*) and in mice (*Ptcl2b*) (GenBank Accession Nos. AB214500 and AB214501, respectively) [12]. Using RT-PCR and exon junction microarrays, *PTCH12b* was demonstrated to be expressed in a brain- and heart-specific fashion [12]. The nucleotide sequence of and adjacent to exon12b was relatively conserved in humans and in mice, especially around the 3′-end of the exon (Fig. 1A). Since premature termination codons (PTCs) were identified in both exons, they are expected to encode proteins truncated just after the sterol-sensing domain (Fig. 1B), whose function in PTCH remains elusive [16]. The splicing regulatory element, UGCAUG, reported to be phylogenetically and spatially conserved in introns that flank the brain-enriched alternative exons [17] was found in the intron regions upstream and downstream of exon 12b in both species (Fig. 1C), supporting the hypothesis that this element is a critical component for tissue-specific splicing events. We next investigated whether exon 12b was also preferentially

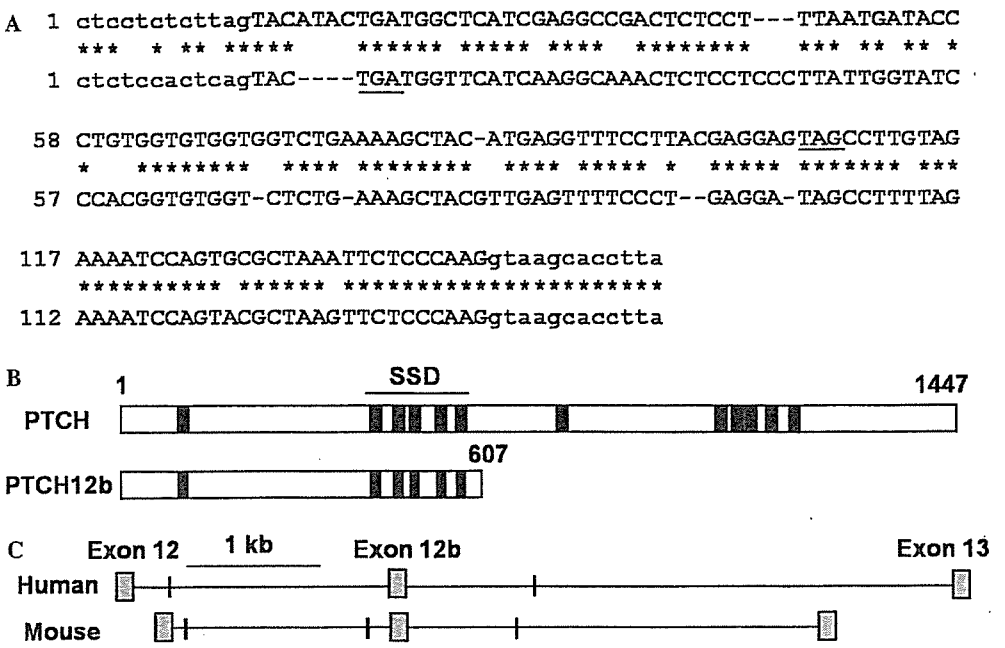

Fig. 1. Exon 12b and flanking splicing elements are conserved in humans and in mice. (A) Alignment of human (upper) and murine (lower) exon 12b and surrounding sequences. Upper- and lowercase letters indicate the exon and intron sequences, respectively. Nucleotides are numbered arbitrarily. Conserved nucleotides are marked by asterisks. In-frame stop codons are underlined. (B) PTCH protein isoforms. Numbers refer to amino acid positions relative to the first methionine of PTCH (NM_000264). Transmembrane domains are indicated by filled boxes. The region containing the 2nd to 6th transmembrane domains comprises the sterol-sensing domain (SSD). (C) Location of UGCAUG hexamers near exon 12b. The location of hexamers is indicated by small vertical thick lines.

expressed in the mouse brain and heart. In adult mice, *Ptc1* (12b−) was more or less expressed in various tissues. However, the *Ptc12b* isoform (12b+) was specifically expressed in the brain and in the heart, particularly in the cerebellum, but not in other tissues, such as the testis and the liver (Fig. 2A). To investigate the expression pattern in the mouse embryo, we performed whole mount *in situ* hybridization. *Ptc12b* was also expressed in the brain and in the heart (Fig. 2B), indicating some role yet to be identified in the development of these tissues. The specificity of the result was confirmed by the negative staining with the sense probe. Taken together, these results imply that the tissue-specific expression of this isoform is evolutionarily conserved.

PTCH12b is expressed in some medulloblastoma tissues and cell lines

Individuals with NBCCS are at high risk of medulloblastomas, which are primitive neuroectodermal tumors. Since medulloblastoma commonly arises in the cerebellum where *PTCH12b* is specifically expressed, we next addressed the question if this isoform is expressed in medulloblastoma cell lines and tissues. Out of 5 medulloblastoma cell lines analyzed, I-23 expressed very high level of *PTCH12b*. None of the 9 non-medulloblastoma cell lines expressed *PTCH12b*. Interestingly, it was also expressed in two out of two medulloblastoma tissues we examined, indicating that this isoform plays a role in the formation of medulloblastoma (Fig. 3A).

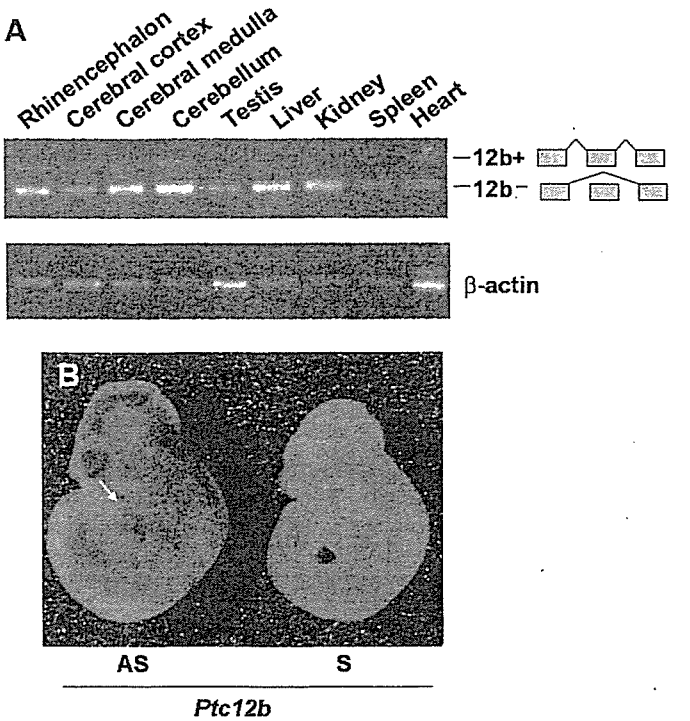

Fig. 2. Tissue-specific expression of *Ptc12b* in mice. (A) Total RNAs obtained from a panel of mouse tissues were subjected to RT-PCR with β-actin as an internal control. A forward primer for exon 11 and a reverse primer for exon 14 were synthesized and used for RT-PCR. All tissues were obtained from a 1-month-old mouse. (B) Whole mount *in situ* hybridization on mouse embryos. Digoxigenin-labeled RNA probes were synthesized in both orientations, sense (S) and antisense (AS), and used on embryos at E10.5. The arrow indicates the position of the heart.

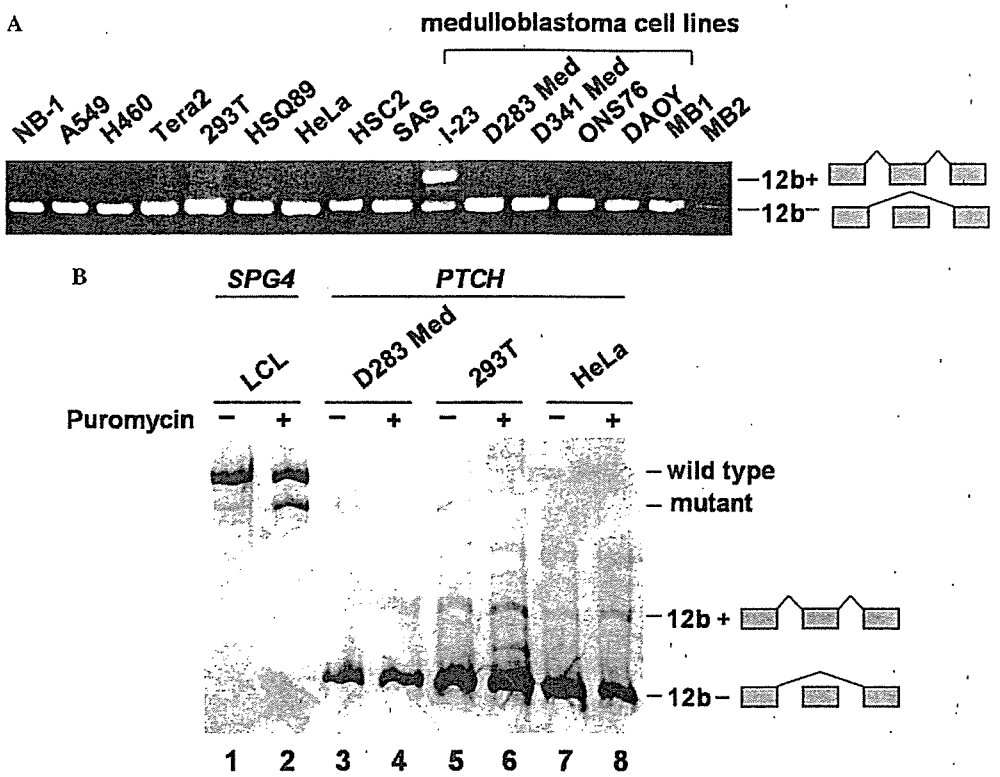

Fig. 3. Expression of exon12b in human cell lines and medulloblastomas. (A) RT-PCR analysis was performed using specific primers for exon 11 and exon 13. RNAs extracted from various cell lines and medulloblastoma samples (MB1, MB2) were used as templates. (B) *PTCH12b* is subjected to NMD to a small extent. Cell lines indicated at the top were grown in the presence or absence of 100 μg/ml puromycin for 6 h. Total RNA was extracted and subjected to RT-PCR. The RT-PCR products were run on a 3.5% polyacrylamide gel to emphasize the difference in size between transcripts from wild type allele and mutant allele of the *SPG4* gene.

PTCH12b isoform undergoes NMD to a small extent

It is known that spliced transcripts with PTCs, such as *Ptc12b* or *PTCH12b*, can potentially activate transcript degradation via the process of nonsense-mediated mRNA decay (NMD) [18]. NMD is important for the removal of PTC-containing transcripts encoding nonfunctional or potentially dominant negative proteins. In order to investigate this possibility, D283 Med, 293T, and HeLa cells, which express barely detectable levels of *PTCH12b*, were cultured in the presence or absence of an NMD inhibitor, puromycin, and subjected to RT-PCR as described above. A lymphoblastoid cell line (LCL) established from a patient in which a PTC is created due to the mutation in the *SPG4* gene (unpublished data by H. U., K. F. and T. M.) was employed as a positive control for NMD. Compared with the positive control where the levels of the transcript containing PTC were markedly increased upon the treatment with puromycin (Fig. 3B, lane 2, mutant), the transcripts of *PTCH12b* were only marginally elevated upon the treatment (Fig. 3B, lanes 4, 6, and 8). Similar results were obtained using another NMD inhibitor, cycloheximide (data not shown). This implies that this isoform undergoes NMD to a limited extent and is already expressed at low abundance independently of NMD in most tissues.

PTCH12b functions as a dominant negative isoform

We performed a functional analysis of PTCH12b using a GLI-responsive luciferase reporter in I-23 medulloblastoma cells. The binding of Shh to its receptor activates a signaling cascade that ultimately leads to an increased activity of the GLI family of transcription factors. The luciferase activities were suppressed when I-23 cells were transfected with plasmids for PTCH, but not with a plasmid for PTCH12b, consistent with PTCH being a suppressive component of the Shh receptor. This also implies that there is a basal level of leakage activity of Smo that excess PTCH prevents in the apparent absence of Shh. However, this suppression by PTCH was relieved when cotransfected with a plasmid for PTCH12b (Fig. 4A). Taken together, these results imply that the PTCH12b protein has a dominant negative effect on PTCH. In order to investigate the subcellular localizations, PTCH12b, as well as PTCH, both tagged with myc at their N-terminal ends, was expressed in HeLa cells and stained with an anti-myc antibody followed by confocal microscopy. PTCH was mainly localized in cytoplasmic vesicular structures as previously reported [19], and no significant difference in localization was observed between PTCH and PTCH12b (Fig. 4B and C). Therefore, it is unlikely that the dominant negative function of PTCH12b is due to its subcellular localization dis-

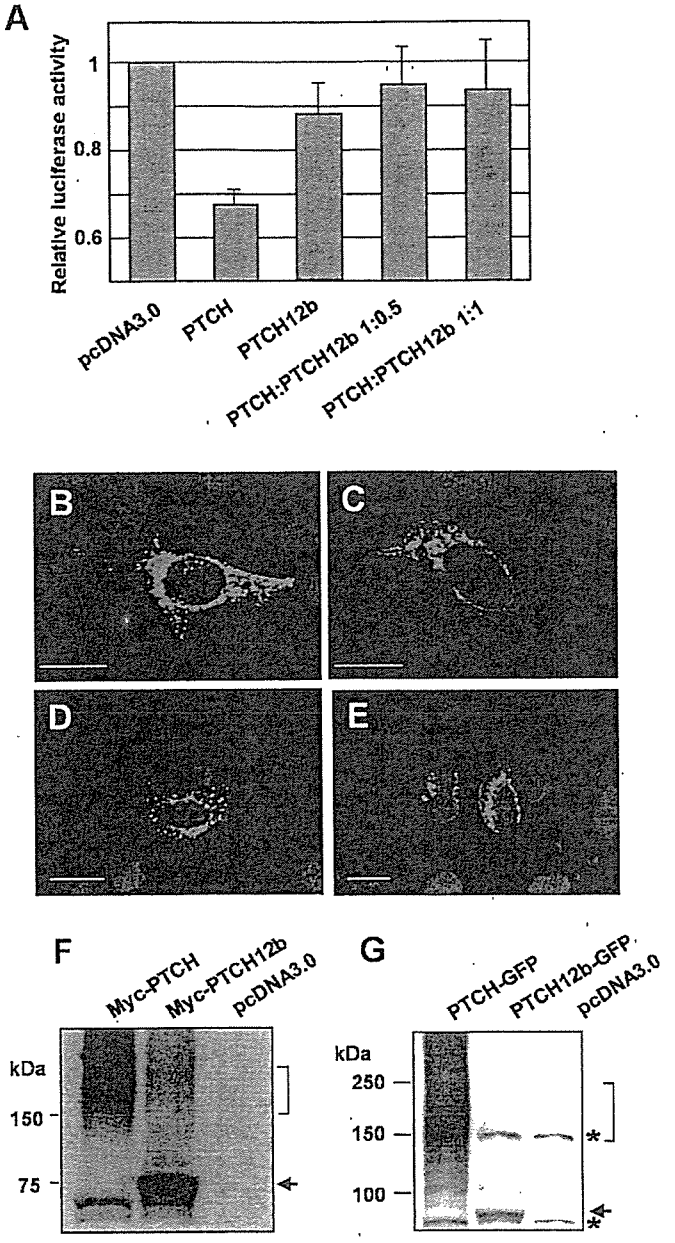

Fig. 4. Functional analysis of *PTCH12b*. (A) I-23 cells were transfected with various combinations of expression plasmids indicated at the bottom, together with a construct for a GLI-responsive luciferase reporter, 8 × GLI-Luc. Twenty-four hours after the transfection, cells were harvested and subjected to a luciferase assay. Shown are the representative data obtained in two independent experiments with triplicates in each experiment. (B–E) Subcellular localization of PTCH proteins. The expression patterns of myc-tagged (B and C) and EGFP-tagged (D and E) PTCH (B and D) or PTCH12b (C and E) in HeLa cells were examined using confocal microscopy. The nuclei were counterstained with Hoechst33342. Bar, 20 μm. (F and G) Western blotting was performed using protein samples obtained from the HeLa cells described above. Anti-c-myc (F) and anti-GFP (G) antibodies were used as a primary antibody. Asterisks indicate non-specific bands.

tinct from PTCH. Similar results were obtained when the both isoforms tagged with enhanced green fluorescent protein (EGFP) at their C-terminal ends were expressed (Fig. 4D and E). Comparative levels of protein expressions of both PTCH and PTCH12b with expected sizes were confirmed by Western blotting (Fig. 4F and G), indicating that the stability of the PTCH12b protein is similar to that of PTCH.

Discussion

Exon 12b in the human *PTCH* gene is conserved in mice and expressed in a brain- and heart-specific manner in both species. According to a recent report by Pan et al., alternative exons with the potential to introduce PTCs upon exon inclusion are not usually conserved between humans and mice [20], suggesting some biological significance of exon 12b.

The precise mechanism of how Ptc12b/PTCH12b functions as a dominant negative isoform remains to be elucidated. Recently, two mutant forms of the Ptc1 protein, G509V and 1130X, have been reported to be dominant negative forms, at least in *Drosophila* [21–23]. Whereas 1130X accumulated strongly along the plasma membrane, G509V and wild type Ptc1 protein localized mainly in the cytoplasmic vesicles, indicating that their mode of action is different [22,23]. Our isoform localized in the cytoplasm. We failed to detect a significant difference in the subcellular localization between PTCH and PTCH12b. It would be interesting to see the *in vivo* function of Ptc12b/PTCH12b using animal models.

The important question would be whether truncated PTCH proteins generally function in a dominant negative manner, because most of the mutations found in patients with NBCCS lead to the truncation of the PTCH protein due to the frameshift or nonsense mutations [24,25]. *Ptc1*$^{-/-}$ mice are embryonic lethal due to the failure of neural tube closure and abnormal development of the heart [26]. Therefore, if truncated PTCH proteins are generally dominant negatives, then the patients with NBCCS should have a phenotype similar to that of *Ptc1*$^{-/-}$ mice, which is not the case. There are at least three explanations regarding this issue. First, mRNA with a frameshift or nonsense mutation may be expressed less than the wild type through NMD-dependent and/or independent mechanisms [20]. Second, at least truncated proteins with a large C-terminal deletion are unlikely to function as a dominant negative. Third, the sensitivity to the perturbation of SHH signaling may be species dependent. For example, mutations in the *SHH* gene are found in some of the children with autosomal dominant holoprosencephaly [27,28], whereas a phenotype resembling human holoprosencephaly is found in *Shh*$^{-/-}$ mice, but not in *Shh*$^{+/-}$ mice [29].

Synthesis of large amounts of C-terminally truncated polypeptides encoded by PTC-containing mRNA is avoided by a splicing- and translation-dependent NMD. Therefore, we wondered why *Ptc12b*/*PTCH12b* is expressed at high levels in certain tissues. Since NMD inhibition resulted in a limited amount of increase in expression of *PTCH12b*, we concluded that this isoform is already present at low levels independently from NMD in most tissues,

and that in the brain and some of the medulloblastomas it is abundantly expressed through a mechanism distinct from the inhibition of NMD. This conclusion is not surprising considering the recent report that only a fraction of PTC-introducing AS events are significantly regulated by NMD [20].

Although a relatively low frequency (10–20%) of sporadic medulloblastomas carry *PTCH* mutations [8], microarray analysis revealed that almost all medulloblastomas with desmoplastic histology are characterized by activation of the SHH signaling pathway [30]. Given the dominant negative function of PTCH12b and the detection of this isoform in the cerebellum and medulloblastoma, it is intriguing to speculate that *PTCH12b* plays an important role in the development of medulloblastoma. In our experiment, 1 out of 5 medulloblastoma cell lines expressed this isoform, whereas 2 out of 2 medulloblastoma tissues expressed this isoform. This may reflect the recent report that Shh activity is down-regulated in cultured medulloblastoma cells [31]. Tumor-specific AS is not a rare event based on a genome-wide computational screen [32]. However, the functional significance of respective protein isoforms generated by these ASs in oncogenesis has yet to be clarified. In NBCCS patients, 65 out of 132 *PTCH* mutations (49%) are localized in the second half of the protein (exon 13 or more downstream). Interestingly, in sporadic medulloblastomas, 16 out of 23 mutations (70%) are found in this region [33], implying that the gene structure encoding *PTCH12b* is more frequently preserved in sporadic medulloblastomas. Although more cases are needed to be investigated, consideration of not only the total expression levels of *PTCH* but also the expression of this particular *PTCH* isoform may help classify medulloblastomas and predict the clinical outcome of the children with medulloblastoma. Lastly, it should be noted that 3% of the individuals with NBCCS are known to have cardiac fibromas [34] and the heart is another tissue where *PTCH12b* is expressed.

Acknowledgments

We thank Mayu Yamazaki-Inoue for her technical support, and Kayoko Saito for preparing the manuscript. This work was supported by the Naito Foundation and Grants for Cancer Research from the Ministry of Health, Labour and Welfare and a Grant-in-Aid for Scientific Research and the Budget for Nuclear Research from the Ministry of Education, Culture, Sports, Science and Technology.

References

[1] P.W. Ingham, A.P. McMahon, Hedgehog signaling in animal development: paradigms and principles, Genes Dev. 15 (2001) 3059–3087.

[2] R.L. Johnson, A.L. Rothman, J. Xie, L.V. Goodrich, J.W. Bare, J.M. Bonifas, A.G. Quinn, R.M. Myers, D.R. Cox, E.H. Epstein Jr., M.P. Scott, Human homolog of *patched*, a candidate gene for the basal cell nevus syndrome, Science 272 (1996) 1668–1671.

[3] H. Hahn, C. Wicking, P.G. Zaphiropoulous, M.R. Gailani, S. Shanley, A. Chidambaram, I. Vorechovsky, E. Holmberg, A.B. Unden, S. Gillies, K. Negus, I. Smyth, C. Pressman, D.J. Leffell, B. Gerrard, A.M. Goldstein, M. Dean, R. Toftgard, G. Chenevix-Trench, B. Wainwright, A.E. Bale, Mutations of the human homolog of *Drosophila patched* in the nevoid basal cell carcinoma syndrome, Cell 85 (1996) 841–851.

[4] R.J. Gorlin, Nevoid basal-cell carcinoma syndrome, Medicine (Baltimore) 66 (1987) 98–113.

[5] J.E. Ming, M.E. Kaupas, E. Roessler, H.G. Brunner, M. Golabi, M. Tekin, R.F. Stratton, E. Sujansky, S.J. Bale, M. Muenke, Mutations in PATCHED-1, the receptor for SONIC HEDGEHOG, are associated with holoprosencephaly, Hum. Genet. 110 (2002) 297–301.

[6] M.R. Gailani, M. Stahle-Backdahl, D.J. Leffell, M. Glynn, P.G. Zaphiropoulos, C. Pressman, A.B. Undén, M. Dean, D.E. Brash, A.E. Bale, R. Toftgård, The role of the human homologue of *Drosophila patched* in sporadic basal cell carcinomas, Nat. Genet. 14 (1996) 78–81.

[7] A.B. Undén, E. Holmberg, B. Lundh-Rozell, M. Stahle-Backdahl, P.G. Zaphiropoulos, R. Toftgård, I. Vorechovsky, Mutations in the human homologue of *Drosophila patched* (*PTCH*) in basal cell carcinomas and the Gorlin syndrome: different in vivo mechanisms of PTCH inactivation, Cancer Res. 56 (1996) 4562–4565.

[8] C. Raffel, R.B. Jenkins, L. Frederick, D. Hebrink, B. Alderete, D.W. Fults, C.D. James, Sporadic medulloblastomas contain *PTCH* mutations, Cancer Res. 57 (1997) 842–845.

[9] P. Kogerman, D. Krause, F. Rahnama, L. Kogerman, A.B. Undén, P.G. Zaphiropoulos, R. Toftgård, Alternative first exons of *PTCH1* are differentially regulated *in vivo* and may confer different functions to the PTCH1 protein, Oncogene 21 (2002) 6007–6016.

[10] T. Shimokawa, F. Rahnama, P.G. Zaphiropoulos, A novel first exon of the *Patched1* gene is upregulated by Hedgehog signaling resulting in a protein with pathway inhibitory functions, FEBS Lett. 578 (2004) 157–162.

[11] K. Nagao, M. Toyoda, K. Takeuchi-Inoue, K. Fujii, M. Yamada, T. Miyashita, Identification and characterization of multiple isoforms of a murine and human tumor suppressor, *patched*, having distinct first exons, Genomics 85 (2005) 462–471.

[12] K. Nagao, N. Togawa, K. Fujii, H. Uchikawa, Y. Kohno, M. Yamada, T. Miyashita, Detecting tissue-specific alternative splicing and disease-associated aberrant splicing of the *PTCH* gene with exon junction microarrays, Hum. Mol. Genet. 14 (2005) 3379–3388.

[13] T. Miyashita, Y. Okamura-Oho, Y. Mito, S. Nagafuchi, M. Yamada, Dentatorubral pallidoluysian atrophy (DRPLA) protein is cleaved by caspase-3 during apoptosis, J. Biol. Chem. 272 (1997) 29238–29242.

[14] M. U, T. Miyashita, Y. Ohtsuka, Y. Okamura-Oho, Y. Shikama, M. Yamada, Extended polyglutamine selectively interacts with caspase-8 and -10 in nuclear aggregates, Cell Death Differ. 8 (2001) 377–386.

[15] Y. Shikama, M. U, T. Miyashita, M. Yamada, Comprehensive studies on subcellular localizations and cell death-inducing activities of eight GFP-tagged apoptosis-related caspases, Exp. Cell Res. 264 (2001) 315–325.

[16] P.E. Kuwabara, M. Labouesse, The sterol-sensing domain: multiple families, a unique role? Trends Genet. 18 (2002) 193–201.

[17] S. Minovitsky, S.L. Gee, S. Schokrpur, I. Dubchak, J.G. Conboy, The splicing regulatory element, UGCAUG, is phylogenetically and spatially conserved in introns that flank tissue-specific alternative exons, Nucleic Acids Res. 33 (2005) 714–724.

[18] J.A. Holbrook, G. Neu-Yilik, M.W. Hentze, A.E. Kulozik, Nonsense-mediated decay approaches the clinic, Nat. Genet. 36 (2004) 801–808.

[19] J. Taipale, M.K. Cooper, T. Maiti, P.A. Beachy, Patched acts catalytically to suppress the activity of Smoothened, Nature 418 (2002) 892–896.

[20] Q. Pan, A.L. Saltzman, Y.K. Kim, C. Misquitta, O. Shai, L.E. Maquat, B.J. Frey, B.J. Blencowe, Quantitative microarray profiling provides evidence against widespread coupling of alternative splicing

with nonsense-mediated mRNA decay to control gene expression, Genes Dev. 20 (2006) 153–158.
[21] R.L. Johnson, L. Milenkovic, M.P. Scott, In vivo functions of the patched protein: requirement of the C terminus for target gene inactivation but not Hedgehog sequestration, Mol. Cell 6 (2000) 467–478.
[22] A.J. Zhu, L. Zheng, K. Suyama, M.P. Scott, Altered localization of *Drosophila* Smoothened protein activates Hedgehog signal transduction, Genes Dev. 17 (2003) 1240–1252.
[23] G.R. Hime, H. Lada, M.J. Fietz, S. Gillies, A. Passmore, C. Wicking, B.J. Wainwright, Functional analysis in *Drosophila* indicates that the NBCCS/PTCH1 mutation G509V results in activation of smoothened through a dominant-negative mechanism, Dev. Dyn. 229 (2004) 780–790.
[24] C. Wicking, S. Shanley, I. Smyth, S. Gillies, K. Negus, S. Graham, G. Suthers, N. Haites, M. Edwards, B. Wainwright, G. Chenevix-Trench, Most germ-line mutations in the nevoid basal cell carcinoma syndrome lead to a premature termination of the PATCHED protein, and no genotype-phenotype correlations are evident, Am. J. Hum. Genet. 60 (1997) 21–26.
[25] K. Fujii, Y. Kohno, K. Sugita, M. Nakamura, Y. Moroi, K. Urabe, M. Furue, M. Yamada, T. Miyashita, Mutations in the human homologue of *Drosophila patched* in Japanese nevoid basal cell carcinoma syndrome patients, Hum. Mutat. 21 (2003) 451–452.
[26] L.V. Goodrich, L. Milenković, K.M. Higgins, M.P. Scott, Altered neural cell fates and medulloblastoma in mouse patched mutants, Science 277 (1997) 1109–1113.
[27] E. Belloni, M. Muenke, E. Roessler, G. Traverso, J. Siegel-Bartelt, A. Frumkin, H.F. Mitchell, H. Donis-Keller, C. Helms, A.V. Hing, H.H. Heng, B. Koop, D. Martindale, J.M. Rommens, L.C. Tsui, S.W. Scherer, Identification of Sonic hedgehog as a candidate gene responsible for holoprosencephaly, Nat. Genet. 14 (1996) 353–356.
[28] E. Roessler, E. Belloni, K. Gaudenz, P. Jay, P. Berta, S.W. Scherer, L.C. Tsui, M. Muenke, Mutations in the human Sonic Hedgehog gene cause holoprosencephaly, Nat. Genet. 14 (1996) 357–360.
[29] C. Chiang, Y. Litingtung, E. Lee, K.E. Young, J.L. Corden, H. Westphal, P.A. Beachy, Cyclopia and defective axial patterning in mice lacking Sonic hedgehog gene function, Nature 383 (1996) 407–413.
[30] S.L. Pomeroy, P. Tamayo, M. Gaasenbeek, L.M. Sturla, M. Angelo, M.E. McLaughlin, J.Y. Kim, L.C. Goumnerova, P.M. Black, C. Lau, J.C. Allen, D. Zagzag, J.M. Olson, T. Curran, C. Wetmore, J.A. Biegel, T. Poggio, S. Mukherjee, R. Rifkin, A. Califano, G. Stolovitzky, D.N. Louis, J.P. Mesirov, E.S. Lander, T.R. Golub, Prediction of central nervous system embryonal tumour outcome based on gene expression, Nature 415 (2002) 436–442.
[31] K. Sasai, J.T. Romer, Y. Lee, D. Finkelstein, C. Fuller, P.J. McKinnon, T. Curran, Shh pathway activity is down-regulated in cultured medulloblastoma cells: implications for preclinical studies, Cancer Res. 66 (2006) 4215–4222.
[32] Z. Wang, H.S. Lo, H. Yang, S. Gere, Y. Hu, K.H. Buetow, M.P. Lee, Computational analysis and experimental validation of tumor-associated alternative RNA splicing in human cancer, Cancer Res. 63 (2003) 655–657.
[33] E. Lindström, T. Shimokawa, R. Toftgård, P.G. Zaphiropoulos, PTCH mutations: distribution and analyses, Hum. Mutat. 27 (2006) 215–219.
[34] D.G. Evans, E.J. Ladusans, S. Rimmer, L.D. Burnell, N. Thakker, P.A. Farndon, Complications of the naevoid basal cell carcinoma syndrome: results of a population based study, J. Med. Genet. 30 (1993) 460–464.